Available online at www.sciencedirect.com

ScienceDirect

Geochimica et Cosmochimica Acta 74 (2010) 1417–1435

Geochimica et Cosmochimica Acta

www.elsevier.com/locate/gca

Tracing the metasomatic and magmatic evolution of continental mantle roots with Sr, Nd, Hf and and Pb isotopes: A case study of Middle Atlas (Morocco) peridotite xenoliths

Nadine Wittig [a,b,*], D. Graham Pearson [a], Svend Duggen [b,c], Joel A. Baker [d], Kaj Hoernle [c]

[a] *Arthur Holmes Isotope Geology Laboratory, Department of Earth Sciences, Durham University, South Road, Durham, DH1 3LE, United Kingdom*

[b] *Danish Lithosphere Centre, Øster Voldgade 10, 1350 Copenhagen K, Denmark*

[c] *Leibniz Institute of Marine Sciences, IFM-GEOMAR, Division Dynamics of the Ocean Floor, Wischhofstraße. 1-3, 24148 Kiel, Germany*

[d] *School of Geography, Environment and Earth Sciences, Victoria University of Wellington, P.O. Box 600, Wellington, New Zealand*

Received 10 September 2009; accepted in revised form 23 October 2009; available online 10 November 2009

Abstract

We studied clinopyroxenes from spinel-facies peridotite xenoliths sampled by the Quaternary intra-plate volcanism of the Middle Atlas (Morocco) and present new trace element and Sr–Nd–Hf isotope data. However, we focus in particular on Pb isotope data and $^{238}U/^{204}Pb$ and $^{232}Th/^{204}Pb$ ratios of these clinopyroxenes. This data allows us to investigate: (a) the timing of metasomatic events, (b) the prevalence and persistence of elevated $^{238}U/^{204}Pb$, $^{232}Th/^{238}U$ and $^{232}Th/^{204}Pb$ in continental mantle roots and (c) the $^{238}U/^{204}Pb$ and $^{232}Th/^{204}Pb$ composition of putative basaltic melts generated from such metasomatised sub-continental lithospheric mantle (SCLM).

Incompatible trace element concentrations in these clinopyroxenes are elevated, marked by high-field strength element depletion and fractionated elemental ratios (e.g., U/Nb, Zr/Hf) most consistent with enrichment due to carbonatitic liquids. Sr, Nd and Hf isotopes have an affinity to HIMU.

U, Th and Pb abundances in the clinopyroxenes generally exceed estimates of primitive mantle clinopyroxene. Pb isotope compositions of these clinopyroxenes are radiogenic and vary between $^{206}Pb/^{204}Pb = 19.93–20.25$, $^{207}Pb/^{204}Pb = 15.63–15.66$ and $^{208}Pb/^{204}Pb = 39.72–40.23$. These Pb isotope systematics result in generally negative $\Delta 7/4$ but positive $\Delta 8/4$; setting these samples distinctly apart from typical HIMU. These Pb isotope compositions are also distinct from the associated host volcanic rocks. $^{238}U/^{204}Pb$ and $^{232}Th/^{204}Pb$ of these clinopyroxenes, which range from 26 to 81 and 136 to 399, respectively, are elevated and more extreme than estimates of MORB- and HIMU-source mantle.

The Pb isotope evolution of the clinopyroxenes suggests that the metasomatic enrichment is younger than 200 Ma, which discounts the volcanic activity due to the opening of the Atlantic and the onset of the collision of the African and Eurasian plates as processes generating the lithophile element and isotope composition of this continental mantle root. Instead, the enrichment is thought to be associated with the Quaternary intra-plate volcanism in the Middle Atlas. However, the erupted mafic melts have unradiogenic Pb isotopes and lower $^{238}U/^{204}Pb$, $^{232}Th/^{204}Pb$ and $^{232}Th/^{238}U$ relative to the clinopyroxene and do not seem to have equilibrated with the clinopyroxenes. The high Th abundances and the high $^{232}Th/^{238}U$ also suggest that the metasomatism was due to carbonatitic liquids.

* Corresponding author. Present address: GeoZentrum Nordbayern, Endogene Geodynamik, Friedrich-Alexander Universität, Schlossgarten 5, D-91054 Erlangen, Germany. Tel.: +49 9131 85 26 065; fax: +49 9131 85 29 295.

E-mail addresses: wittig@geol.uni-erlangen.de, hobbes@steinlaus.me.uk (N. Wittig).

doi:10.1016/j.gca.2009.10.048

When literature data for Pb isotopes in mantle minerals are considered, the Pb isotope range of Archean, Proterozoic and Phanerozoic continental mantle roots is remarkable in that they are similar to the convecting mantle. This observation does not support the existence of sub-continental lithospheric mantle with high $^{238}U/^{204}Pb$ and $^{232}Th/^{204}Pb$ for long periods of time. Consequently, the narrow range of Pb isotopes in SCLM worldwide suggests that only the youngest metasomatic events are recorded by incompatible elements such as U, Th and Pb. Numerical modelling of putative magmas generated from Middle Atlas SCLM by fractional, non-modal melting calculations yield extremely high $^{238}U/^{204}Pb$ and $^{232}Th/^{204}Pb$ ratios. For example, pure SCLM magmas generated from 0.5% to 10% melting are anticipated to have $^{232}Th/^{204}Pb$ ratios exceeding those known from terrestrial basalts.

1. INTRODUCTION

Sub-continental lithospheric mantle (SCLM) is often invoked as a versatile isotopic reservoir in order to explain the isotopic idiosyncrasies in the global mid-ocean ridge basalt (MORB) and ocean island basalt record (OIB) (Hawkesworth et al., 1983; McKenzie and O'Nions, 1983, 1995; Hassler and Shimizu, 1998; Hanan et al., 1999; O'Reilly et al., 2006, 2008). In addition, SCLM is frequently regarded as an important contributor to intraplate continental volcanism (Chauvel and Jahn, 1984; Turner and Hawkesworth, 1995; Shaw et al., 2007). The Sr–Nd isotope variation of peridotitic SCLM, although encompassing a wide range of compositions within individual suites, generally resembles that of MORB and OIB (Pearson and Nowell, 2002). Furthermore, the mantle samples with the most extreme Sr–Nd isotope characteristics have negligible Nd concentrations relative to plausible magma source regions (Pearson and Nowell, 2002). Consequently, Sr–Nd isotope variations do not appear to be particularly diagnostic in evaluating potential recycling and incorporation of SCLM into terrestrial volcanism. In comparison, emerging Nd–Hf isotope data suggests remarkable variation in lithospheric minerals that is distinct from the tightly correlated OIB range in certain, carbonatite/hydrous fluid-metasomatised xenoliths suites (Bizimis et al., 2003, 2007; Wittig et al., 2006; Shaw et al., 2007). Therefore, the combination of Hf and Nd isotopes may yield a powerful, although yet to be tested tool in detecting incorporation of SCLM into terrestrial volcanism (Pearson and Nowell, 2002; Wittig et al., 2006, 2007). However, high-εHf clinopyroxene separates generally originate from highly infertile harzburgites that are unlikely to participate in mantle melting. Fertile lherzolites, however, seem to maintain coupled Sr–Nd–Hf isotopes indistinguishable from the bulk of oceanic basalts (e.g., Shaw et al., 2007; Wittig et al., 2007).

The U/Pb and Th/Pb isotope systems are among the most versatile analytical tools available for investigating the evolution of geological material (Tera, 2006). Recently, methodological advances render the accurate and precise analysis of Pb isotopes possible in samples with low Pb abundances (Woodhead et al., 1995; Galer, 1999; Abouchami et al., 2000; Thirlwall, 2000, 2002). Yet presently, the data available for samples recovered from continental mantle roots is scarce (~400 analysis of individual clinopyroxene separates; Wittig et al. 2009a, Fig. 1) relative to the analyses of volcanic rocks derived from the convecting mantle (see compilation by Stracke et al., 2003 yielding ca. 2450 samples). One of the challenges of interpreting Pb isotope analyses in low level material such as mantle clinopyroxene comes from the high abundance of "anthropogenic", enriched-mantle-like Pb in the environment that

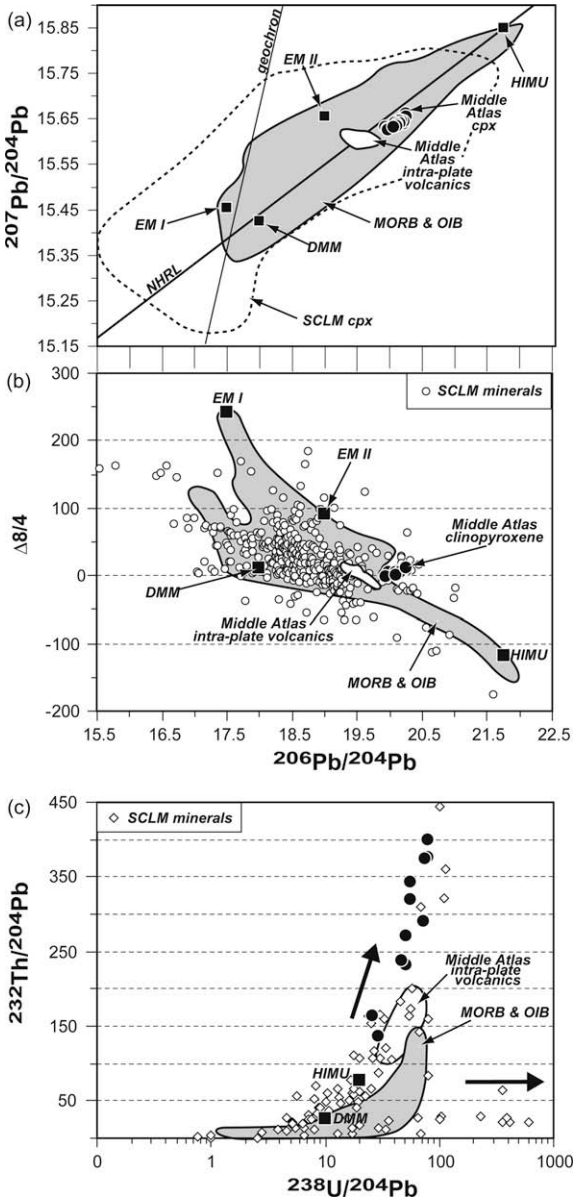

has the potential to dominate $^{206}Pb/^{204}Pb$ and $^{207}Pb/^{204}Pb$ in mantle minerals if leaching techniques are inadequate (Wittig et al., 2009a). The compiled Pb isotope data of SCLM minerals suggest that: (a) SCLM minerals exhibit somewhat greater $^{207}Pb/^{204}Pb$ isotope variation as compared to the convecting mantle (Fig. 1), (b) $^{206}Pb/^{204}Pb > 20.5$ ("true" HIMU, high mu [$^{238}U/^{204}Pb$]) is virtually absent and (c) enriched mantle (EM) Pb isotope ratios appear to be particularly dominant although Sr isotopes in these samples do not resemble enriched mantle. It is important to recognize that all recovered leachates from mantle minerals have EM-like Pb isotopes and that the corresponding clinopyroxenes have very different Pb isotopes that, in most cases, do not resemble the EM component. Further discussion of the Pb isotope systematics of mantle clinopyroxene–leachate pairs can be found in Wittig et al. (2009a).

In mantle clinopyroxenes, parent/daughter elemental ratios of the Sr, Nd, Hf and Pb isotope systems are also rarely provided (e.g., $\leqslant$140 for $^{238}U/^{204}Pb$ and $^{232}Th/^{204}Pb$, Fig. 1). In contrast to the Hf (^{176}Lu $t_{1/2}$ ~37.2 Gyr), Os (^{187}Re $t_{1/2}$ ~42.3 Gyr), Sr (^{87}Rb $t_{1/2}$ ~47.5 Gyr) and Nd (^{147}Sm $t_{1/2}$ ~106 Gyr) isotope systems, the half-lives of ^{232}Th ($t_{1/2}$ ~14.3 Gyr) and in particular ^{238}U ($t_{1/2}$ ~4.6 Gyr) are considerably shorter. These relatively short half-lives may facilitate the understanding of several aspects in the evolution of SCLM. For example, the short half-lives of U and Th result in rapid isotopic in-growth of Pb isotopes in metasomatically enriched mantle clinopyroxene over relatively short periods of time (i.e. tens of Myr) that is not observed in Sr, Nd or Hf isotope systematics and may help in determining the relative timing of metasomatic enrichment. Moreover, Th and U show contrasting behavior during metasomatic enrichment in hydrous and some carbonatitic liquids (Bell and Tilton, 2001) that percolate through the SCLM. As such, hydrous and carbonatitic fluids may result in highly fractionated $^{232}Th/^{238}U$ ratios (κ) in mantle minerals that are distinctly lower (e.g., Wittig et al., 2007) or higher (this study) than estimates for depleted MORB-mantle (DMM, $\kappa \sim 2.5$) and Bulk Silicate Earth (BSE, $\kappa \sim 3.4$, Galer and O'Nions, 1985). In contrast, percolating silicate melts are less likely to impose fractionated $^{232}Th/^{238}U$ on the SCLM and are thought to impart κ within the typical range of DMM and BSE. Hence, $^{232}Th/^{238}U$ in mantle clinopyroxene may distinguish metasomatic enrichment due to hydrous (i.e. very low κ) versus carbonatitic fluids (i.e. very low to elevated κ).

During partial melting of fertile upper mantle the incompatibilities of Th and U are broadly similar (Wood et al., 1999; Landwehr et al., 2001) whereas Pb is assumed to be somewhat more compatible in silicates (Hart and Gaetani, 2006). As such, mafic melts might possess elevated Th/Pb and U/Pb ratios in comparison to the residual peridotite. Given the unusually large range of $^{232}Th/^{204}Pb$ and $^{238}U/^{204}Pb$ in clinopyroxene recovered from SCLM (Fig. 1) small-degree melting of lithospheric mantle may be traceable by utilizing the $^{238}U/^{204}Pb$ (μ), $^{232}Th/^{204}Pb$ (ω) and $^{232}Th/^{238}U$ (κ) in these minerals.

The samples from the Middle Atlas presented here were previously discussed strictly in the context of evaluating methodological procedures and the Pb isotope and μ, ω and κ systematics of clinopyroxene–leachate pairs (Wittig et al., 2009a). In this contribution, we present new clinopyroxene trace element abundances and Sr, Nd and Hf isotope data and focus on the geological interpretation of the new U, Th and Pb elemental data and $^{238}U/^{204}Pb$, $^{232}Th/^{204}Pb$ and $^{232}Th/^{238}U$ of these samples. We explore the potential of Pb isotopes and elevated $^{238}U/^{204}Pb$, $^{232}Th/^{204}Pb$ and $^{232}Th/^{238}U$ in (a) constraining the timing of SCLM metasomatism, (b) contemplating the prevalence and persistence of high-μ and high-ω signatures in the SCLM and (c) show the anticipated range of μ and ω in basaltic melts if the Middle Atlas SCLM was to participate in mantle melting.

Fig. 1. Panel (a) shows $^{207}Pb/^{204}Pb$ versus $^{206}Pb/^{204}Pb$ of subcontinental lithospheric mantle minerals (SCLM; dashed field, Cohen et al., 1984; Hamelin and Allègre, 1988; Stolz and Davies, 1988; Walker et al., 1989; Galer and O'Nions, 1989; Ben Othman et al., 1990; Meijer et al., 1990; Mukasa et al., 1991; Porcelli et al., 1992; Tatsumoto et al., 1992; Kramers et al., 1993; Pearson et al., 1993; Carlson and Irving, 1994; Hauri et al., 1994; Carignan et al., 1996; Lee et al., 1996; Rosenbaum et al., 1997; Baker et al., 1998; Brandon et al., 1999; Mukasa and Shervais, 1999; Ionov et al., 2002; Santos et al., 2002; Witt-Eickschen et al., 2003; Choi et al., 2005; Shaw et al., 2007; Wittig et al., 2007; Wittig et al., 2009a). Also shown is the range of oceanic basalts (MORB and OIB; grey field; Stracke et al. (2003) and references therein, $n = 2450$) in addition to typical mantle endmember compositions (black squares; HIMU, EMI, EMII, DMM after Hofmann, 1997). NHRL denotes the Northern Hemisphere Reference Line after Hart (1984). The Middle Atlas clinopyroxenes (black circles) and volcanic rocks (Duggen et al., 2009) are shown for comparison. Panel (b) shows $\Delta 8/4$ versus $^{206}Pb/^{204}Pb$ of the same data sets as in (a) except here the individual SCLM clinopyroxene data points are shown. $\Delta 8/4$ denotes the deviation of $^{208}Pb/^{204}Pb$ from the NHRL as defined by Hart (1984). Note the unusual combination of positive $\Delta 8/4$ and radiogenic $^{206}Pb/^{204}Pb$ found in the Middle Atlas SCLM clinopyroxenes. References are the same as in panel (a). Panel (c) shows $^{232}Th/^{204}Pb$ versus $^{238}U/^{204}Pb$ of oceanic basalts, HIMU and DMM, the Middle Atlas volcanic rocks and the literature compilation of SCLM minerals (white diamonds). Arrows denote the two main trends exhibited in the global μ and ω record of SCLM clinopyroxenes. References are the same as in panel (a). The Middle Atlas clinopyroxenes are highlighted as black circles.

2. ANALYTICAL METHODS

Trace element concentrations and Sr–Nd–Hf–Pb isotope ratios were determined on primary chrome diopside (>0.7 mm) in the ultra-clean laboratories at the Northern Centre for Isotopic and Elemental Tracing (NCIET, Department of Earth Sciences, Durham University) and the Danish Lithosphere Centre (Copenhagen University).

2.1. Removing the ubiquitous grain-boundary contamination from mantle clinopyroxenes by HCl leaching

The grain-boundary contamination of mantle minerals has been studied in detail by Bedini and Bodinier (1999) and Wittig et al. (2009a). Bedini and Bodinier (1999) reported extreme grain-boundary contamination of lithophile trace

elements. The leaching experiments by Wittig et al. (2009a) showed that up to 90% of the Pb associated with the clinopyroxene–leachate pairs are found on the grain surfaces and not in the crystal lattice and also illustrated the extreme variability in crystal- and grain-boundary-hosted Pb isotopes, $^{238}U/^{204}Pb$, $^{232}Th/^{204}Pb$ and $^{232}Th/^{238}U$ that is *not* due to U, Th and Pb fractionation during HCl leaching. In fact, the grain boundaries typically yield Pb isotopes akin to anthropogenic Pb, which lies intermediate between the enriched mantle components (EM I and EM II, Wittig et al., 2009a). For clinopyroxenes from a single websteritic sample (GP101, Pearson and Nowell, 2004), which is used in Durham as an in-house clinopyroxene standard for lithophile isotopes (Pearson and Nowell, 2004), leaching acids and crystals also exhibit well correlated and yet highly variable Pb, Sr, Nd and Hf isotopes (Wittig et al., 2009a).

For trace element and Pb–Sr isotope determinations, the Middle Atlas clinopyroxenes were leached with ultra-pure reagents either (a) for 1 h with cold 2N HCl and were repeatedly rinsed with 18.2 Ω MQ water (Milli-Q©) or (b) for 1 h with cold 2N HCl and repeatedly rinsed with MQ water followed by an additional leaching step lasting for 2 h using hot 6N HCl. The residue was then repeatedly rinsed with MQ water. Replicate digestions from these two leaching procedures show that Pb isotope ratios reproduce within the 100 ppm proposed by Baker et al. (2004) for Pb double-spike techniques. This good agreement of Pb isotope ratios from two different leaching procedures highlights the validity of the leaching procedures (Wittig et al., 2009a).

For Hf and Nd isotope determinations the leaching procedures recommended by Wittig et al. (2009a) were applied. The Middle Atlas clinopyroxenes were washed in MQ water in a heated ultrasonic bath for 1 h. After removing the MQ water and rinsing of the crystals repeatedly, two leaching steps with 2N HCl and 6N HCl (30 min at 120 °C) were performed. In between leaching steps, the crystals were thoroughly rinsed (3×) with MQ water. The excellent Nd isotope reproducibility of replicate digestions of the Middle Atlas clinopyroxenes (Fig. 2) shows that the leaching procedures applied were suitable in removing the ubiquitous grain-boundary contamination associated with mantle minerals. The leaching procedures used here do not result in fractionation of parent and daughter elements (e.g. Lu from Hf) during sample preparation (Wittig et al., 2009a).

2.2. Trace element determination of mantle clinopyroxenes

Analyses of Middle Atlas clinopyroxene separates were performed on ~10 mg aliquots. Following the removal of the leaching acid, the minerals were repeatedly rinsed with

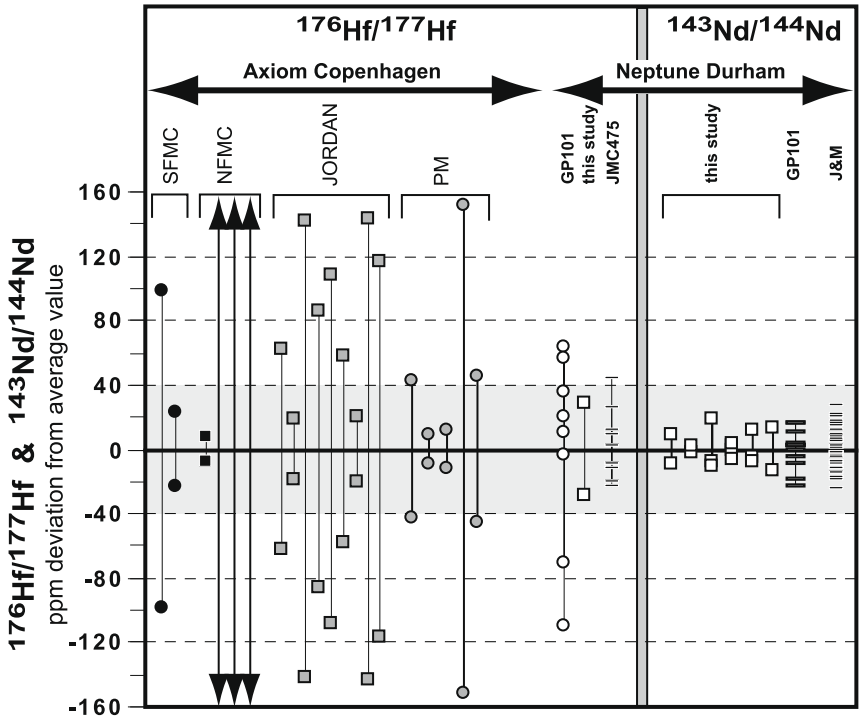

Fig. 2. Reproducibility of Hf and Nd isotope replicate digestions of mantle clinopyroxenes shown as $^{176}Hf/^{177}Hf$ and $^{143}Nd/^{144}Nd$ deviation (in ppm) from the average value comparing Middle Atlas samples (open squares) to literature data. Also shown are Hf and Nd isotope mass spectrometry standards JMC475 and J&M and "Axiom" and "Neptune" denote the type of MC-ICP-MS used in Copenhagen and Durham, respectively. Samples from the literature originate from the southern (SFMC, black circle) and northern French Massif Central (NFMC, black squares, ultra-depleted, Wittig et al., 2007), Jordan (grey squares, Shaw et al., 2007) and the Pyrenean Massif (PM, grey circle, Wittig 2006). GP101 is an in-house control clinopyroxene sample (open circle [Hf] and bar [Nd]) from Beni Bousera (Pearson and Nowell, 2004) that was prepared and analysed together with the Middle Atlas samples. In contrast to the clinopyroxenes from the French Massif Central, Jordan, Pyrenean Massif and Beni Bousera, which are marked by heterogeneous Hf concentrations and isotopes (Pearson and Nowell, 2004; Wittig 2006; Shaw et al., 2007; Wittig et al., 2007) the samples from the Middle Atlas appear to be isotopically homogeneous.

Table 1
Trace element abundances (ppm) of Middle Atlas mantle clinopyroxenes.

	Atl-3A	Atl-3B	Atl-3C	Atl-3E	Atl-3F	Atl-3I	Atl-3K	Atl-3L	Atl-3T	Atl-3U	Atl-3V	GP101	RSD%	W2	RSD%	BHVO1	RSD%	AGV-1	RSD%	BE-N	RSD%	BIR-1	RSD%	NBS688	RSD%
Parts per million																									
Rb	0.065	0.013	0.005	0.040	0.025	0.006	0.004	0.019	0.032	0.143	0.062	0.0407	4.83	19.7	1.24	9.35	2.78	66.1	2.24	47.3	0.16	0.245	4.34	1.96	0.43
Ba	0.648	0.384	0.275	0.372	0.488	0.131	0.112	1.44	0.558	1.47	0.712	0.179	1.16	176	0.66	137	0.43	1226	0.70	1053	0.49	7.57	2.22	173	0.01
Th	0.290	1.47	1.43	1.19	0.892	0.254	0.704	1.23	2.217	1.20	0.181	0.201	1.46	2.23	1.16	1.25	0.17	6.42	0.07	11.0	1.66	0.0355	1.99	0.338	1.05
U	0.065	0.340	0.318	0.247	0.229	0.053	0.139	0.226	0.376	0.249	0.030	0.0609	1.26	0.499	1.84	0.416	0.85	1.91	1.15	2.46	1.53	0.0130	0.03	0.270	2.62
Nb	0.399	2.04	0.188	0.281	0.512	0.584	0.232	1.60	6.34	3.02	4.03	0.288	1.31	7.63	1.59	19.3	1.00	14.4	1.30	117	0.79	0.803	12.9	5.42	0.31
Ta	0.004	0.161	0.012	0.011	0.021	0.085	0.013	0.178	0.339	0.185	0.232	0.0478	1.12	0.494	1.20	1.26	1.01	0.922	0.77	6.20	1.04	0.0555	3.82	0.392	2.53
La	6.4	22.6	8.47	8.83	8.46	5.4	8.98	11.33	24.1	9.31	6.0	1.32	1.04	10.6	0.70	15.4	0.29	38.1	0.10	82.6	0.73	0.639	0.89	5.19	0.30
Ce	17.7	68.7	13.2	12.6	7.2	15.5	20.2	27.5	80.2	19.0	21.7	3.29	1.00	22.8	0.63	37.4	0.46	67.3	0.49	151	0.38	1.94	0.44	11.8	0.45
Pr	2.21	8.90	1.26	1.24	0.657	2.46	2.32	3.82	12.19	2.50	3.64	0.454	1.26	3.14	0.94	5.63	0.98	8.86	1.46	18.4	0.70	0.399	0.89	1.86	0.50
Sr	151	299	80.2	87.0	107	160	128	137	398	118	130	37.90	0.83	201	0.57	405	0.44	655	0.64	1547	0.41	113	0.80	174	0.28
Nd	7.25	32.79	4.15	4.40	2.83	11.22	7.52	15.28	51.40	9.94	16.04	2.56	1.67	13.7	0.80	26.1	0.78	33.7	1.96	71.4	0.17	2.54	0.17	8.89	0.38
Pb	0.146	0.437	0.259	0.218	0.210	0.0730	0.179	0.266	0.445	0.208	0.0762	0.520	0.89	7.52	1.01	2.16	4.09	36.1	0.04	4.01	0.67	2.85	3.32	2.62	2.45
Zr	9.26	22.0	11.1	13.6	12.8	43.3	12.3	14.0	37.6	16.8	19.6	9.56	2.76	90.6	1.38	174	0.94	228	0.75	272	1.11	14.8	0.54	55.1	0.65
Hf	0.297	0.741	0.368	0.450	0.386	0.609	0.407	0.361	0.764	0.317	0.370	0.334	0.84	2.42	1.60	4.41	0.80	5.10	1.18	5.75	0.23	0.595	1.43	1.51	1.40
Sm	0.946	4.53	0.837	0.874	0.806	2.39	1.09	2.82	8.91	1.81	3.11	0.732	0.93	3.38	1.45	6.24	0.84	5.95	2.11	12.5	0.63	1.14	2.37	2.45	0.03
Eu	0.301	1.37	0.298	0.313	0.307	0.715	0.367	0.849	2.55	0.549	0.934	0.182	1.82	1.09	1.26	2.01	0.63	1.77	0.60	3.79	0.97	0.501	1.69	0.976	1.45
Gd	0.916	3.34	1.01	1.04	1.11	2.10	1.11	2.30	6.28	1.51	2.55	0.607	2.49	3.86	1.35	6.52	1.03	4.79	0.87	10.0	0.75	2.01	1.65	3.14	0.79
Tb	0.161	0.431	0.181	0.180	0.198	0.291	0.191	0.329	0.849	0.219	0.360	0.0939	1.69	0.643	1.73	0.981	0.94	0.679	0.10	1.33	0.80	0.407	2.43	0.552	0.38
Dy	1.05	2.80	1.16	1.11	1.30	1.53	1.21	1.77	4.49	1.22	1.97	0.562	1.30	3.83	1.15	5.31	1.12	3.48	0.49	6.36	1.27	2.54	1.39	3.31	1.96
Ho	0.229	0.547	0.252	0.237	0.282	0.286	0.263	0.341	0.834	0.238	0.385	0.120	1.36	0.796	0.74	0.993	0.36	0.684	0.52	1.11	0.51	0.575	1.11	0.749	0.28
Y	6.53	14.8	7.33	6.64	8.28	8.96	7.21	8.96	29.9	6.68	11.0	3.45	1.69	22.3	1.14	27.3	1.07	20.1	0.05	30.5	0.42	16.9	0.64	21.4	0.66
Er	0.628	1.56	0.700	0.648	0.776	0.692	0.725	0.857	2.07	0.606	0.981	0.319	1.43	2.14	1.00	2.42	1.14	1.76	0.72	2.50	1.30	1.64	1.90	2.10	0.34
Tm	0.0975	0.210	0.110	0.0981	0.119	0.0991	0.110	0.126	0.305	0.0919	0.143	0.0514	1.52	0.331	1.62	0.344	3.29	0.269	0.79	0.329	0.22	0.259	2.18	0.336	1.68
Yb	0.588	1.50	0.674	0.599	0.718	0.569	0.668	0.752	1.80	0.560	0.871	0.297	1.10	2.08	1.66	2.04	1.32	1.68	3.96	1.88	1.32	1.69	0.71	2.12	0.63
Lu	0.0940	0.199	0.107	0.0943	0.114	0.088	0.105	0.117	0.199	0.088	0.135	0.0458	0.96	0.337	1.21	0.306	1.16	0.270	3.14	0.279	3.30	0.281	0.50	0.350	0.40
Th/U	4.46	4.33	4.50	4.80	3.90	4.83	5.06	5.45	5.90	4.84	6.07	—	—	—	—	—	—	—	—	—	—	—	—	—	—
Nd/Pb	49.6	74.9	16.0	20.2	13.5	153.8	42.0	57.5	115.6	47.9	210.5	—	—	—	—	—	—	—	—	—	—	—	—	—	—
Lu/Hf	0.32	0.27	0.29	0.21	0.29	0.14	0.26	0.32	0.26	0.28	0.37	—	—	—	—	—	—	—	—	—	—	—	—	—	—
Sm/Nd	0.13	0.14	0.20	0.20	0.28	0.21	0.14	0.18	0.17	0.18	0.19	—	—	—	—	—	—	—	—	—	—	—	—	—	—
Rb/Sr	0.00043	0.000044	0.000061	0.00046	0.00023	0.000038	0.000028	0.00014	0.000080	0.0012	0.00048	—	—	—	—	—	—	—	—	—	—	—	—	—	—
primitive mantle-normalized																									
$[U/Nb]_N$	5.0	5.1	51.4	26.8	13.6	2.7	18.3	4.3	1.8	2.5	0.2	—	—	—	—	—	—	—	—	—	—	—	—	—	—
$[Zr/Hf]_N$	0.9	0.8	0.8	0.8	0.9	2.0	0.8	1.1	1.4	1.5	1.5	—	—	—	—	—	—	—	—	—	—	—	—	—	—
$[Lu/Hf]_N$	0.8	0.9	0.8	1.1	0.8	1.7	0.9	0.7	0.9	0.9	0.7	—	—	—	—	—	—	—	—	—	—	—	—	—	—

Notes: Primitive mantle after Sun and McDonough (1989). Average values and RSD% of international standard reference material ($n = 2$, except W2 $n = 8$) run together with the Middle Atlas clinopyroxenes are also given. Average values and RSD% of the Durham in-house lithophile isotope clinopyroxene standard GP101 result from one digestion and 3 analyses. U, Th and Pb of the Middle Atlas clinopyroxenes are taken from Wittig et al. (2009a).

MQ and subsequently digested with 29N HF/16N HNO_3 and 12N HCl until the residue was in complete solution utilizing ultra-pure reagents and procedures of Ottley et al. (2003). All trace element abundances were blank-corrected. The reproducibility of the international standard material (BHVO1 [$n = 2$], W2 [$n = 8$], BE-N [$n = 2$], BIR-1 [$n = 2$], AGV-1 [$n = 2$], NBS688 [$n = 2$]) and the in-house mantle clinopyroxene standard GP101 that were run together with the Atlas clinopyroxenes is better than 5% for all trace elements reported in Table 1 and in excellent agreement with accepted values.

Malarkey et al. (2008) have highlighted substantial trace element abundance variability of primary clinopyroxenes on thin-section-scale (e.g., 134–300 ppm Sr) in samples Atl-3V and Atl-3U that is independent of the textural occurrence of these minerals. This data was prepared using highly accurate and precise micro-milling techniques developed by Charlier et al. (2006) and Harlou et al. (2009). Sr isotope systematics from the same Middle Atlas clinopyroxenes are relatively homogenous and in agreement with the results of this study (Malarkey et al., 2008). This trace element variability has been confirmed by initial laser-ablation inductively coupled plasma mass spectrometry (ICP-MS) measurements of a sub-set of Middle Atlas xenoliths (Wittig, 2006). The reported trace element heterogeneity of the studied clinopyroxenes is the rational for this study to prepare trace element measurements from bulk clinopyroxene separates via solution ICP-MS in order to achieve robust and representative trace element budgets hosted in primary clinopyroxenes that can be used in the melt modeling. The reproducibility of Atlas clinopyroxene replicate digestions ($n = 2$) for U/Pb, Th/Pb and Th/U is <0.9%, 1.8% and 1.3% (Wittig et al., 2009a).

2.3. Chemical separation and analysis of Nd and Hf isotopes of mantle clinopyroxenes

Hf and Nd isotope data have been prepared in the ultra-clean Arthur Holmes Isotope Geology Laboratory at Durham University using flux fusion methods similar to those described by Bizzarro et al. (2003), Ulfbeck et al. (2003) and Wittig et al. (2007). After leaching approximately 100 mg of carefully hand-picked clinopyroxenes were dried and sandwiched between two layers of ~170 mg of ultra-pure $LiBO_2$ in pre-ignited high-purity graphite crucibles (0.6 mL). The samples were then fused at ~1100 °C in a furnace and the molten samples were poured into 22 mL Savillex Teflon vials containing 15 mL of Teflon distilled 2N HCl. The samples were heated and agitated to facilitate dissolution of the glass pellets in the 2N HCl. Once the samples were completely dissolved, the solutions were loaded through filter paper onto Biorad 15 mL columns containing AG50Wx8 cation exchange resin. The sample matrix was eluted using 12 mL 1N HCl and 2N HCl, respectively. Hf was collected in 15 mL of 2N HNO_3 and evaporated, whereas Nd was eluted using 20 mL of 6N HCl. The Nd cut was also evaporated, fluxed with three drops of 16N HNO_3 and taken up in 3% HNO_3 for mass spectrometry. The Hf cut was taken up in 1 mL of 1N HCl and reloaded on a second set of Biorad columns with AG50Wx8 cation exchange resin. The loading solution and 3 mL of 1N HCl/1N HF was collected and dried down before the samples were fluxed with three drops of 16N HNO_3 and taken up in 0.5 mL of a 3% HNO_3/HF mixture (9.5:0.5) for mass spectrometry.

Hf and Nd isotope measurements were performed using a Thermo Finnigan Neptune multi-collector ICP-MS at NCIET in Durham. Details of mass spectrometry procedures are given in Pearson and Nowell (2004) and Nowell et al. (2003). Hf standard JMC475 ($n = 13$) was analyzed together with the Middle Atlas clinopyroxenes in two sessions and yielded an average $^{176}Hf/^{177}Hf = 0.282147 \pm 11$ (2σ) resulting in a reproducibility of ~38 ppm (Fig. 2). For Nd isotope measurements, pure and Sm-doped J&M standard solutions (total $n = 51$) were run in five sessions. The average $^{143}Nd/^{144}Nd$ was 0.511109 ± 12 (2σ) resulting in a reproducibility of 24 ppm (Fig. 2). These results for JMC475 and J&M are in excellent agreement with published values (e.g., Nowell et al., 2003; Pearson and Nowell, 2004). Hf and Nd blanks were <100 pg. We also performed replicate digestions of the websteritic in-house "control" mantle clinopyroxene GP101 (Pearson and Nowell, 2004). These digestions yielded a mean $^{176}Hf/^{177}Hf$ and $^{143}Nd/^{144}Nd$ of 0.282547 ± 4 and 0.512207 ± 2 resulting in an excellent Hf and Nd isotope reproducibility of 32 and 122 ppm ($n = 11$, $n = 8$), respectively, compared to previously published data from mantle clinopyroxene, particularly for $^{143}Nd/^{144}Nd$ (Fig. 2). Replicate digestions of Middle Atlas clinopyroxene for Pb–Nd–Hf isotope analyses (see Section 2.4 and Wittig et al., 2009a) indicate that leaching, digestion and mass spectrometry procedures were adequate. These data also strongly suggests that this mantle clinopyroxene population, despite showing highly variable trace element abundances (Malarkey et al., 2008) is marked by limited variability in Hf and Nd isotopes (this study, Table 2).

2.4. Chemical separation and analysis of Sr and Pb isotopes of mantle clinopyroxenes

Approximately 100 mg of hand-picked clinopyroxene were digested in the ultra-clean laboratory of the Danish Lithosphere Centre at Copenhagen University. The leaching acid was removed by pipetting and the minerals were repeatedly rinsed with MQ water before ultra-pure 29N HF/16N HNO_3 and 7N HCl were used to digest the minerals. Pb was separated from major and trace elements by a double-pass anion exchange procedure (Baker et al., 2004). Chemical separation of Pb was carried out on acid-leached single-use polypropylene pipette tips (1 mL volume) as mini-columns using approximately 5 mm of AG-50-W-x8 100–200 mesh anion exchange resin. The sample matrix, including Sr, was eluted with three reservoirs of 1N HBr before Pb was collected in 7N HCl. Total procedural Pb blanks recorded during the course of 2 years are generally ~4 pg and never exceeded 12 pg. This is regarded as insignificant, even when the low Pb abundances of mantle clinopyroxene are considered. The reproducibility of the international Pb isotope standard SRM 981 is 89, 96 and 97 ppm for $^{206}Pb/^{204}Pb$ (16.9405 ± 0.0027), $^{207}Pb/^{204}Pb$

Table 2
Rb–Sr, Sm–Nd and Lu–Hf isotope data of Middle Atlas mantle clinopyroxenes.

	$^{87}Rb/^{86}Sr$	$^{87}Sr/^{86}Sr$	2se	$^{147}Sm/^{144}Nd$	$^{143}Nd/^{144}Nd$	2se	εNd	$^{176}Lu/^{177}Hf$	$^{176}Hf/^{177}Hf$	2se	εHf	ΔεHf
Atl-3A	0.0013	0.703350	±9	0.081	0.512861	±10	+4.4	0.0450	0.283181	±10	+14.5	+6.9
Atl-3A	—	—	—	—	0.512863	±6	+4.4	—	—	—	—	—
Atl-3B	0.00013	0.703400	±9	0.085	0.512812	±12	+3.4	0.0382	0.283263	±6	+17.4	+11.1
Atl-3C	0.00018	0.70330	±1	0.124	0.512902	±4	+5.1	0.0414	0.283295	±14	+18.5	+9.9
Atl-3C	—	—	—	—	0.512915	±6	+5.4	—	—	—	—	—
Atl-3C	—	—	—	—	0.512900	±6	+5.1	—	—	—	—	—
Atl-3E	0.0013	0.70324	±2	0.122	0.512922	±6	+5.5	0.0298	0.283061	±24	+10.2	+1.1
Atl-3E	—	0.70324	±1	—	0.512921	±8	+5.5	—	—	—	—	—
Atl-3E	—	—	—	—	0.512923	±16	+5.6	—	—	—	—	—
Atl-3E	—	—	—	—	0.512918	±6	+5.5	—	—	—	—	—
Atl-3F	0.0067	0.70317	±3	0.176	0.513018	±8	+7.4	0.0419	0.283206	±22	+15.3	+3.6
Atl-3F	—	0.70323	±1	—	—	—	—	—	—		—	—
Atl-3I	0.0001	0.70333	±1	0.131	0.512839	±8	+3.9	0.0204	0.283200	±26	+15.1	+8.2
Atl-3K	0.0001	0.70337	±1	0.089	0.512864	±6	+4.4	0.0368	0.283097	±6	+11.5	+3.9
Atl-3K	—	—	—	—	0.512863	±8	+4.4	—	0.283081	±18	+10.9	+3.3
Atl-3K	—	—	—	—	0.512873	±10	+4.6	—	—	—	—	—
Atl-3L	0.0004	0.70340	±1	0.114	0.512820	±6	+3.6	0.0461	0.283296	±2	+18.5	+12.1
Atl-3L	—	—	—	—	0.512834	±6	+3.8	—	—	—	—	—
Atl-3T	0.0002	0.70339	±1	0.107	0.512813	±4	+3.4	0.0370	0.283297	±12	+18.6	+12.3
Atl-3U	0.0035	0.70338	±8	0.112	0.512839	±6	+3.9	—	—	—	—	—
Atl-3U	—	—	—	—	0.512848	±10	+4.1	—	—	—	—	—
Atl-3V	0.0014	0.70340	±1	0.120	0.512828	±6	+3.7	0.0520	0.283175	±4	+14.3	+7.6
In-house clinopyroxene standard												
GP101	0.0080	0.70854	±1	0.173	0.512207	±2	−8.4	0.0193	0.282547	±4	−8.0	0.0

Notes: εHf and εNd are calculated as the part per 10,000 deviation from present-day Bulk Earth values (Blichert-Toft and Albarede, 1997; Jacobsen and Wasserburg, 1980). $\Delta\varepsilon Hf = \varepsilon Hf - (1.36 \times \varepsilon Nd + 1.63)$ after Johnson and Beard (1993). Parent-isotope ratios were calculated using elemental concentrations given in Table 1. Mean values of replicate digestions of the in-house clinopyroxene standard GP101 for Sr–Hf–Nd isotope ratios are also given ($n = 2$, $n = 11$, $n = 8$, ±2 S.D.).

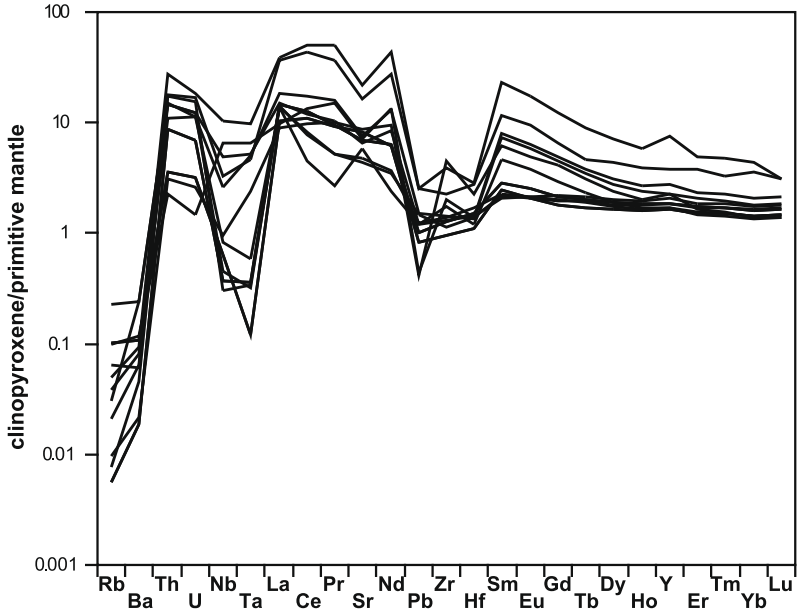

Fig. 3. Primitive-mantle-normalized (Sun and McDonough, 1989) multi-element patterns for clinopyroxenes from spinel-facies Middle Atlas peridotite xenoliths.

(15.4986 ± 0.0030) and $^{208}Pb/^{204}Pb$ (36.7229, ±0.0039, 2σ, $n = 15$). Internal precision for $^{206}Pb/^{204}Pb$, $^{207}Pb/^{204}Pb$ and $^{208}Pb/^{204}Pb$ of Middle Atlas mantle clinopyroxene is <±0.002 2se, ±0.003 2se and ±0.005 2se, respectively, and result in typical double-spike reproducibility ($^{206}Pb/^{204}Pb < 100$ppm, see Baker et al., 2004; Wittig et al. 2009a). Sr was further purified by evaporating the HBr and dissolving the residue in 3N HNO_3 before this solution was loaded onto mini-columns filled with 5 mm Sr-spec resin. Three reservoirs of 3N HNO_3 were eluted before Sr was collected in three reservoirs of MQ water. The Sr-containing MQ water cut was dried down and analyzed by thermal ionization mass spectrometry at the Geological Institute, Copenhagen University.

3. SAMPLES AND RESULTS

This study investigates a suite of peridotite clinopyroxene separates from spinel-facies peridotite xenoliths ($n = 11$) erupted by the Quaternary intra-plate volcanism of the Middle Atlas, Morocco. In general, all samples are porphyroblastic and contain melt pockets that sometimes host minor amounts of relict amphibole and/or spinel (Wittig, 2006). Olivine and clinopyroxene modal abundance (56–90% and 2–23%, respectively), Sc-V and MgO-FeO systematics suggests a variable SCLM composition beneath the Middle Atlas. The samples are more fertile than primitive mantle (PRIMA) with a sub-fraction recording spinel-facies depletion up to 25 to 30% at ~2 GPa. Whole rock Os isotope systematics vary between $\gamma Os = +1.8$ and -6.7, whereas PGE (platinum-group element) abundances are marked by Pd-enrichment (Wittig et al., 2008, in press). Al_2O_3 in whole-rocks correlates with Os isotopes; and also Ir, Cu and MgO abundances but these element-element trends deviate from the compositions anticipated for residual mantle. The major element, PGE and Os isotope systematics indicate that modal metasomatism due to the percolation of mafic silicate melts effected this continental root and resulted in the coupled introduction of sulphides and a Al-bearing mineral such as amphibole and/or spinel and clinopyroxene. Consequently, this suite of xenoliths does not preserve information on the age of pristine mantle depletion (Wittig et al., 2008, in press).

Lithophile trace element concentrations in clinopyroxenes are generally enriched relative to PRIMA and marked by comparatively low high-field strength element abundances and fractionated elemental ratios such as U/Nb, Zr/Hf (Table 1 and Fig. 3). Sr, Nd and Hf isotopes are typical for mantle clinopyroxene ($^{87}Sr/^{86}Sr = 0.7031$–0.7034, $\varepsilon Nd = +3.4$ to $+7.4$, $\varepsilon Hf = +10$ to $+19$) and are tightly associated with the mantle array (Table 2, Fig. 4). There is no correlation of $^{87}Rb/^{86}Sr$, $^{147}Sm/^{144}Nd$ and $^{176}Lu/^{177}Hf$ with $^{87}Sr/^{86}Sr$, $^{143}Nd/^{144}Nd$ and $^{176}Hf/^{177}Hf$ (not shown) and the isotopes ratios are within the range anticipated from Bulk Earth and depleted MORB-mantle. In comparison to the host volcanic rocks (Duggen et al., 2009) the mantle clinopyroxenes exhibit similar Sr but more radiogenic Nd isotopes (Fig. 4).

The investigated clinopyroxenes have U, Th and Pb abundances ranging between 0.03 and 0.38 ppm, 0.18 and 2.2 ppm and 0.07 and 0.45 ppm, respectively (Table 1, Wittig et al., 2009a). Apart from Atl-3A, Atl-3I, Atl-3V the majority of clinopyroxenes have U and Th abundances that are equal to, or up to 6 times higher than those of estimated PRIMA clinopyroxene (U ~ 0.08 ppm, Th ~ 0.39 ppm; Fig. 5).

Pb isotope ratios of these clinopyroxenes are radiogenic ($^{206}Pb/^{204}Pb = 19.93$–$20.25$, $^{207}Pb/^{204}Pb = 15.63$–$15.66$ and $^{208}Pb/^{204}Pb = 39.72$–$40.23$; Table 3, Fig. 1 and 6). In comparison to clinopyroxenes from other SCLM, the Pb isotope ratios of the Atlas clinopyroxenes show a remarkably small variation. For example, we have calculated "$^{206}Pb/^{204}Pb$ indices" similar to ΔSr devised by Davidson et al. (2005), by subtracting the solar system initial $^{206}Pb/^{204}Pb$ (9.307;

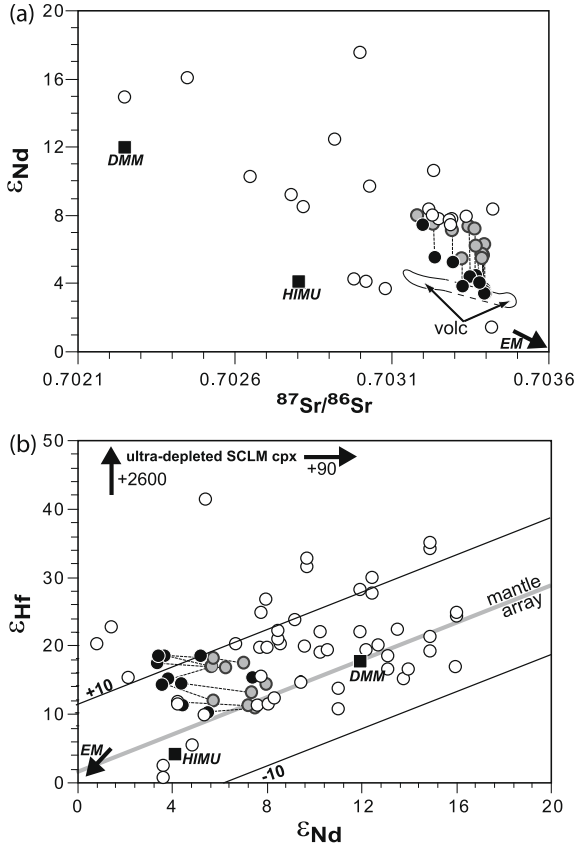

Fig. 4. Plot of εNd versus $^{87}Sr/^{86}Sr$ (a) and εHf versus εNd (b) comparing the Middle Atlas SCLM clinopyroxenes (black circles) to the MORB and HIMU endmember (black squares) in addition to mantle clinopyroxene from the literature (open circles, Bizimis et al., 2003; Shaw et al., 2007; Wittig, 2006; Wittig et al., 2007). 2σ analytical uncertainties are smaller than the symbol size. The mantle array in (b) (present-day and ±10 epsilon units) and εHf are calculated after Johnson and Beard (1993), while εNd is calculated after Blichert-Toft and Albarede (1997). Also shown is the composition of the Middle Atlas SCLM clinopyroxenes 200 Ma (grey circles) connected by dashed tie-lines to the corresponding present-day composition. The back-modelled Sr–Nd–Hf isotope composition at the time of eruption (2 Ma) and 20 Ma cannot be visually resolved from the present-day composition. Also shown is the field for the Sr–Nd isotope composition of the Middle Atlas host volcanic rocks (Duggen et al., 2009).

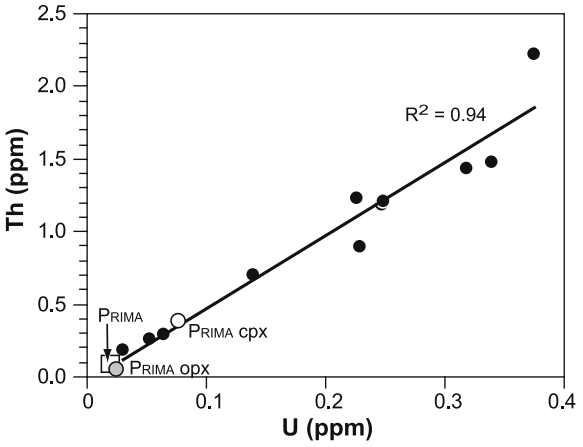

Fig. 5. Th versus U concentrations (ppm) of clinopyroxenes from the Middle Atlas SCLM with respect to estimates of Primitive Mantle (PRIMA, Sun and McDonough, 1989). Also shown are the calculated compositions of PRIMA clinopyroxene and orthopyroxene using modal abundances taken from Walter (2003) and partition coefficients from Witt-Eickschen and O'Neill (2005). Most clinopyroxenes are distinctly more enriched than PRIMA clinopyroxene, and U and Th enrichment appears coupled resulting in a positive correlation (linear model, $R^2 = 0.94$).

Tatsumoto et al., 1973) from the most and least radiogenic $^{206}Pb/^{204}Pb$ for normalization purposes. Then the least radiogenic $^{206}Pb/^{204}Pb$ is subtracted from the most radiogenic $^{206}Pb/^{204}Pb$. For the suite of Middle Atlas clinopyroxenes the most radiogenic sample is Atl-3K ($^{206}Pb/^{204}Pb \sim 20.25$) from which the $^{206}Pb/^{204}Pb$ of sample Atl-3I ($^{206}Pb/^{204}Pb \sim 19.93$) is subtracted yielding the following equation:

$$^{206}Pb/^{204}Pb \text{ index Middle Atlas} = (20.25 - 9.307) - (19.93 - 9.307) = 0.3.$$

The off-cratonic French Massif Central, the orogenic peridotite Pyrenean Massif and cratonic xenoliths from the Tanzanian craton host clinopyroxenes that have distinctly more variable Pb isotopes with "$^{206}Pb/^{204}Pb$ indices" of 2.7, 2.6 and 4.9. The combination of radiogenic Pb and generally positive Δ8/4 (deviation from the Northern Hemisphere Reference Line, NHRL, Hart 1984) renders the Middle Atlas mantle clinopyroxenes dissimilar to oceanic basalts, and also most SCLM minerals (Fig. 1).

The samples have unusually high $^{238}U/^{204}Pb$ (μ, 26–81), $^{232}Th/^{204}Pb$ (ω, 136–399) and $^{232}Th/^{238}U$ (κ, >4.5) with respect to estimates of DMM- and HIMU-mantle (Table 3 and Fig. 6). The Quaternary volcanic rocks from the Middle Atlas that host the mantle xenoliths have distinctly different, and generally less radiogenic Pb and lower μ, ω and κ as compared to the data for the mantle clinopyroxenes presented here (Figs. 1, 6 and 7; Duggen et al., 2009).

4. DISCUSSION

4.1. Evidence for carbonatite metasomatism in Middle Atlas clinopyroxene

The Middle Atlas clinopyroxenes have Lu, Zr and Hf abundances that result in variable and fractionated $[Lu/Hf]_N$ and $[Zr/Hf]_N$ ratios (PRIMA-normalized after Sun and McDonough, 1989) that range between 0.8 to

Table 3
Pb isotope data and μ, ω and κ of clinopyroxene separates from Middle Atlas mantle xenoliths.

	$^{206}Pb/^{204}Pb$	2 se	$^{207}Pb/^{204}Pb$	2 se	$^{208}Pb/^{204}Pb$	2 se	Δ7/4	Δ8/4	$^{238}U/^{204}Pb$ μ	$^{232}Th/^{238}U$ κ	$^{232}Th/^{204}Pb$ ω
Atl-3A	20.089	±2	15.635	±2	39.966	±3	−3.4	5.1	29.5	4.61	136
Atl-3A	20.093	±1	15.638	±2	39.977	±3	−3.1	5.7	—	—	—
Atl-3B	20.176	±2	15.643	±2	40.049	±3	−3.5	2.9	51.6	4.47	231
Atl-3B	20.1745	±7	15.644	±1	40.058	±1	−3.4	4.0	—	—	—
Atl-3C	20.1763	±8	15.640	±1	40.075	±2	−3.8	5.5	80.8	4.65	375
Atl-3E	20.1060	±7	15.635	±1	40.003	±1	−3.5	6.8	75.2	4.96	373
Atl-3E	20.1114	±9	15.636	±1	40.011	±2	−3.5	6.9	—	—	—
Atl-3F	19.9774	±9	15.629	±1	39.828	±2	−2.8	4.8	72.1	4.03	290
Atl-3F	19.9793	±7	15.629	±1	39.831	±1	−2.7	4.9	—	—	—
Atl-3I	19.933	±2	15.632	±3	39.718	±5	−2.0	−0.9	47.5	4.99	237
Atl-3K	20.2499	±8	15.657	±1	40.173	±2	−2.9	6.4	51.7	5.23	271
Atl-3L	20.1831	±8	15.644	±1	40.083	±2	−3.5	5.5	56.6	5.63	319
Atl-3T	20.2456	±8	15.652	±1	40.226	±2	−3.4	12.2	56.3	6.10	343
Atl-3U	20.213	±1	15.642	±2	40.126	±2	−4.0	6.2	79.7	5.00	399
Atl-3U	20.2166	±8	15.643	±1	40.134	±2	−3.9	6.5	—	—	—
Atl-3V	20.104	±2	15.639	±3	39.937	±4	−3.2	0.5	26.0	6.27	163
In-house clinopyroxene standard											
GP101	18.6055	±1	15.680	±1	39.239	±3	17.2	111.8	10.9	3.42	37.2

Notes: Δ7/4 and Δ8/4 taken from Hart, 1984. In-house clinopyroxene standard GP101 taken from Wittig et al. (2009a).

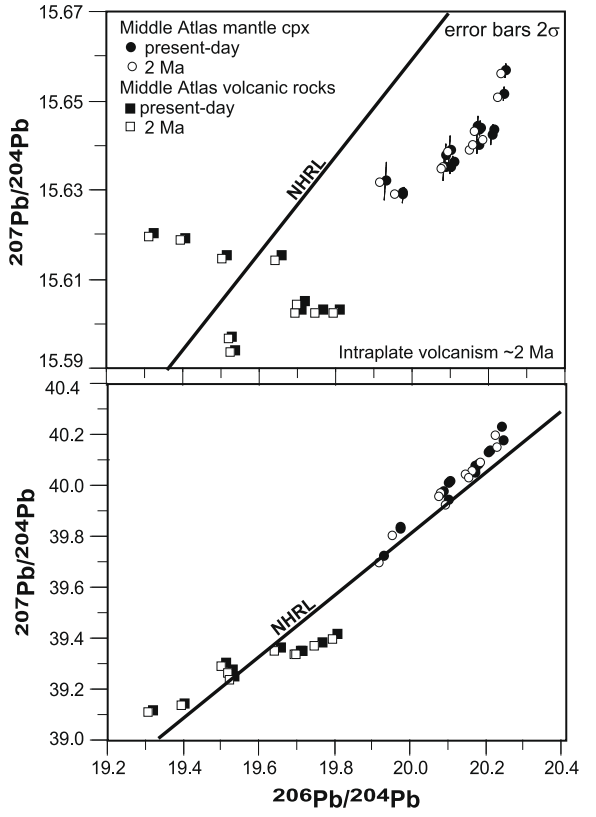

Fig. 6. $^{207}Pb/^{204}Pb$ (a) and $^{208}Pb/^{204}Pb$ (b) versus $^{206}Pb/^{204}Pb$ showing the Middle Atlas mantle clinopyroxene (black circles) together with their host intra-plate volcanic rocks (black squares, Duggen et al., 2009) that erupted ~2 Ma (El Azzouzi et al., 1999). The Pb isotope systematics of the age-corrected samples (open symbols) shows that the currently observed radiogenic Pb of the clinopyroxenes cannot result from interaction with the erupted host volcanic rocks. NHRL denotes the Northern Hemisphere Reference Line after Hart (1984).

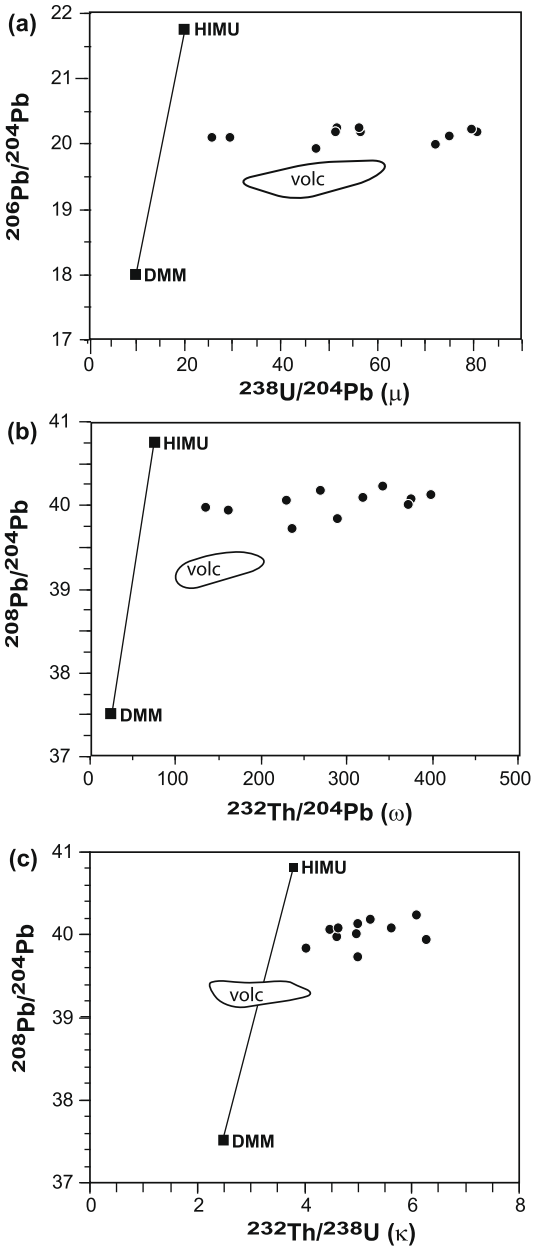

Fig. 7. Panel (a) shows $^{206}Pb/^{204}Pb$ versus $^{238}U/^{204}Pb$, while (b) and (c) show $^{208}Pb/^{204}Pb$ versus $^{232}Th/^{204}Pb$ and $^{208}Pb/^{204}Pb$ versus $^{232}Th/^{238}U$ illustrating the highly elevated parent isotope ratios of the Middle Atlas mantle clinopyroxenes (black circles). These clinopyroxenes exceed estimates for DMM- and HIMU-mantle (black squares, Galer and O'Nions, 1985; Thirlwall, 1997) and basanitic host volcanic rocks (volc; Duggen et al., 2009).

1.7 and 0.8 to 2.0, respectively. These elements are assumed to be among the more resilient elements towards metasomatic enrichment in the SCLM. The Lu/Hf range is only consistent with up to 5% spinel-facies melting (Wittig et al., 2007). Notably, if the least incompatible and relatively immobile rare earth element, Lu, is considered alone, it appears that only one sample (Atl-3I) preserves a record of shallow melting to the extent of ~20%. This suggests that Hf abundances, and all elements more incompatible and/or mobile than Lu, are substantially enriched despite the negative Nb–Ta and Zr–Hf anomalies exhibited by these clinopyroxenes when normalized to primitive mantle (Fig. 3). The high-field strength element depletions and the fractionation of elements with similar incompatibility during melting and metasomatism (e.g. $[U/Nb]_N$, $[Nd/Pb]_N$, $[Zr/Hf]_N$, Table 1 and Fig. 3) exhibited by these clinopyroxenes generally excludes generic basaltic intra-plate melts as well as the host volcanic rocks (Duggen et al., 2009) as the metasomatic agent. Importantly, carbonatites may have extremely variable ratios of these elements (e.g. $[U/Nb]_N = 0.4–81$, $[Nd/Pb]_N = 0.01–5.0$, $[Zr/Hf]_N = 0.08–2.3$, Bell and Tilton, 2001).

Further information regarding the type of metasomatic agent that has influenced the mantle clinopyroxenes can be derived from U, Th and Pb elemental systematics and their Pb isotopes, μ, ω and κ. Volcanic rocks derived from melting of oceanic mantle have a restricted range of $^{232}Th/^{238}U$ (κ) between 2.5 in depleted samples and up to 3.4 in BSE. The partitioning behavior of Th and U into the clinopyroxene crystal lattice is nearly identical (Wood et al., 1999; Landwehr et al., 2001) and therefore metaso-

matic enrichment from the percolation of generic basaltic melts and particularly the host volcanic rocks through the Middle Atlas SCLM can be excluded due to the lower $^{232}Th/^{238}U$ of these mafic lavas relative to the clinopyroxenes (Fig. 7). Elemental ratios of Th and U can also distinguish carbonatitic and hydrous fluids. Typical subduction zone fluids are anticipated to have low Th abundances relative to U and Pb (Bailey and Ragnarsdottir, 1994) thus yielding low $^{232}Th/^{238}U$ and $^{232}Th/^{204}Pb$. Carbonatites have highly variable and often elevated μ, ω and κ (Bell and Tilton, 2001). For example, although $^{238}U/^{204}Pb$, $^{232}Th/^{204}Pb$ and $^{232}Th/^{238}U$ data in carbonatites are not abundant ($n = 35$), these ratios vary between 0.3 to 40, 0.3 to 347 and 0.6 to 77, respectively (Bell and Tilton, 2001). Therefore, the very high Th abundances and $^{232}Th/^{238}U$ of the Middle Atlas clinopyroxenes render hydrous fluids as an unlikely metasomatic agent for generating the most recent enrichment recorded by these clinopyroxenes. These Th and U abundances and $^{238}U/^{204}Pb$, $^{232}Th/^{204}Pb$ and $^{232}Th/^{238}U$ ratios also confirm that the metasomatic agent causing the enrichment of the Middle Atlas SCLM had considerably more variable trace element systematics than putative mafic silicate melts, and that the metasomatic agent may have been carbonatitic liquids. Considering the record of metasomatic enrichment evident in the lithophile trace element systematics of these clinopyroxenes, the Pb, Sr, Nd and Hf isotopes are extremely unlikely to yield information regarding the timing of mantle melting.

In the case of the Middle Atlas SCLM at least two distinct metasomatic events can now be distinguished. An earlier enrichment due to the percolation of silicate melts resulted in the precipitation of amphibole and/or clinopyroxene with spinel, elevated Pd abundances and high Al_2O_3 that are coupled with radiogenic Os isotopes (Wittig et al., in press). However, the observed lithophile trace element systematics in the clinopyroxenes require later metasomatic enrichment due to the interaction with carbonatitic fluids.

4.2. The timing of metasomatism in the Middle Atlas SCLM

It is important to note that the high μ, ω and κ of these samples show no correlation with Pb isotopes and are distinct from typical source mantle of DMM and HIMU (Fig. 7) and the host volcanic rocks from the Middle Atlas (Duggen et al., 2009). The Pb isotope composition of the SCLM clinopyroxenes and the host volcanic rocks do not overlap within the past 2 Myr (Age of volcanism, El Azzouzi et al., 1999, Fig. 6). The knowledge of the Pb isotope ratios and μ, ω and κ systematics of the Atlas mantle clinopyroxenes allows us to relate the evolution of Pb isotopes back in time to other volcanic activity in the region. Below we explore the timing of the youngest metasomatic event that led to the very high μ, ω and κ of the Middle Atlas SCLM clinopyroxenes.

Little is known about the assembly of the continental fragments in the Middle Atlas prior to or during the Variscan. In principle, the metasomatic enrichment of the SCLM beneath the Middle Atlas may have occurred at any time following the initial depletion and coupling of the continental crust to the supporting continental mantle root. Subsequent tectonic events are (a) the Triassic-Jurassic opening of the Atlantic basin, (b) the emplacement of the Central Atlantic Magmatic Province (~200 Ma, Knight et al., 2004; Verati et al., 2005) and (c) the Cenozoic commencement of the collision of the Eurasian and African continental plates. The latter event resulted in the closure and exhumation of the Atlas rift system (Gomez et al., 1998; Ayarza et al., 2005), which could have affected the continental mantle roots substantially. Furthermore, alkaline intra-plate volcanism occurred in the Middle Atlas from the Miocene onwards (El Azzouzi et al., 1999), whereas calc-alkaline volcanism signifies subduction zone activity (~20 Ma) in the western Mediterranean (Duggen et al., 2003, 2008) approximately 400 km to the North. As such, a 200 Myr period during which the metasomatism in the SCLM may have occurred is considered.

The low parent/daughter ratios $^{87}Rb/^{86}Sr$, $^{147}Sm/^{144}Nd$ and $^{176}Lu/^{177}Hf$ of the Middle Atlas clinopyroxenes result in insignificant change of the corresponding isotope ratios when these are modeled 200 Myr back in time (Fig. 4). In contrast, modeling the Pb isotope ratios of representative Atlas mantle clinopyroxene separates (Fig. 8a and b) back in time shows the very rapid and relatively shallow evolution of these samples in $^{207}Pb/^{204}Pb$–$^{208}Pb/^{204}Pb$ space as compared to estimates of the NHRL at the respective times. A first order observation is that the Pb isotopes, when modeled back in time, become less radiogenic than the initial Pb isotope estimates of the solar system (Tatsumoto et al., 1973) after only 1.2–0.6 Gyr. This provides an obvious absolute maximum age for the presence of the elevated μ, ω and κ in these samples. In comparison to estimates of the NHRL 200 Ma, $^{207}Pb/^{204}Pb$ and $^{208}Pb/^{204}Pb$ of these clinopyroxenes are strongly decoupled. $^{207}Pb/^{204}Pb$ remains somewhat associated with the back-modelled NHRL ($\Delta 7/4_{200Ma} = -1.3$ to $+7.5$) whereas $^{208}Pb/^{204}Pb$ lies markedly below the NHRL ($\Delta 8/4_{200Ma} = -29$ to -137). This decoupling of $^{208}Pb/^{204}Pb$ and $^{207}Pb/^{204}Pb$ stems from the extremely high Th abundances in the SCLM clinopyroxenes that are considerably higher than those of U. This leads to ω that is markedly higher than μ and hence very high κ (>4.5). These elevated Th/U ratios drive the back-modeled $^{208}Pb/^{204}Pb$-$^{206}Pb/^{204}Pb$ along a considerably more vertical trend than the MORB and OIB array (i.e. $\kappa_{NHRL} = 3.4$) (Fig. 8b). Thus, the decoupling of $^{208}Pb/^{204}Pb$ and $^{207}Pb/^{204}Pb$ in the Middle Atlas clinopyroxenes do not seem to allow interaction with putative mantle-derived melts formed at ~200 Ma. This strongly suggests that the metasomatic enrichment responsible for the present-day radiogenic Pb isotopes and elevated μ, ω and κ of the Atlas SCLM clinopyroxene occurred much more recently, and does not result from the tectonic events associated with the opening of the Atlantic. Notably, most clinopyroxenes have $^{207}Pb/^{204}Pb$ that is very close to the NHRL when they are back-modeled for no longer than 20 Myr. This result suggests that the SCLM has interacted with highly enriched, carbonatitic liquids (see Section 4.1) that are possibly associated with the mafic intra-plate volcanism, yet isotopically dissimilar to the regionally erupted intra-plate volcanic rocks that host these mantle xenoliths.

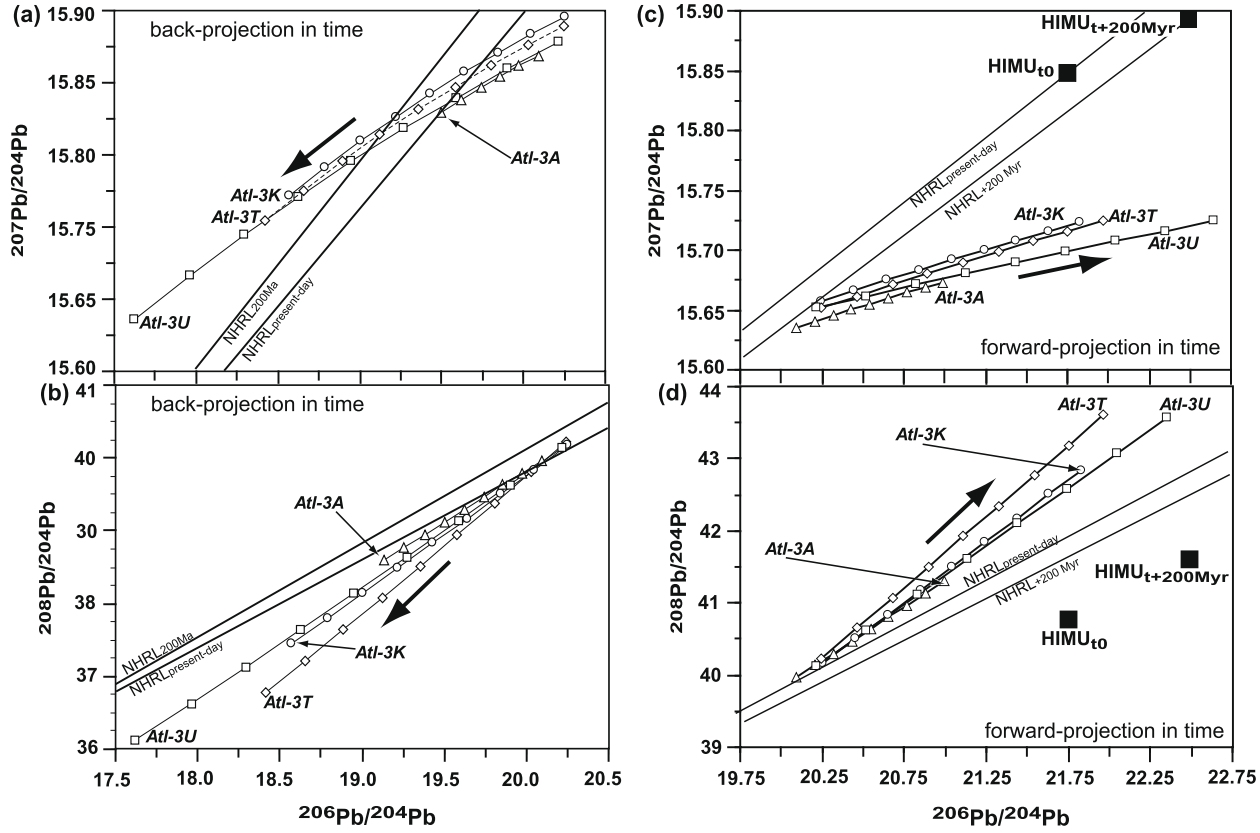

Fig. 8. Evolution of $^{207}Pb/^{204}Pb$ (a, c) and $^{208}Pb/^{204}Pb$ (b, d) versus $^{206}Pb/^{204}Pb$ of representative Middle Atlas mantle clinopyroxene separates (Atl-3A, Atl-3K, Atl-3T, Atl-3U) projected back- and forward in time (200 Myr, 25 Myr steps) using measured μ and ω to calculate corresponding Pb isotope ratios. The NHRL is shown at its present-day composition and also projected back- and forward (200 Myr) using adapted parameters from Thirlwall (1997) for depleted mantle. ^{238}U and ^{232}Th decay constants are taken from Steiger and Jager (1977) in order to calculate Pb isotopes, μ and ω at the respective times. Also shown is the present-day, and forward modeled ($t_{200\ Myr}$) Pb isotope composition of HIMU (c, d).

4.3. Prevalence and persistence of elevated μ and ω SCLM clinopyroxenes

Very few studies have addressed Pb isotope systematics and μ, ω and κ in SCLM clinopyroxene (Galer and O'Nions, 1985; Meijer et al., 1990; Tatsumoto et al., 1992; Wittig et al., 2007, 2009a). However, these ratios can be calculated for a number of additional SCLM portions (Stolz and Davies, 1988; Pearson et al., 1993; Hauri et al., 1994; Baker et al., 1998; Brandon et al., 1999; Mukasa and Shervais, 1999; Ionov et al., 2002; Witt-Eickschen et al., 2003, Fig. 1; Becculuva et al., 2007; Shaw et al., 2007). Several of these publications dealt with samples that also have extreme μ, ω and κ similar to the Middle Atlas SCLM (e.g., Hoggar intra-plate volcanic field, southern French Massif Central, Becculuva et al., 2007; Wittig et al., 2007). Therefore, we assume that the metasomatic enrichment of the Middle Atlas lithosphere does not originate from a particularly unique process and similar enrichment due to the percolation of highly enriched metasomatic agents within the SCLM is relatively common. Allowing for these very high $^{232}Th/^{204}Pb$ and $^{238}U/^{204}Pb$ ratios in SCLM it seems remarkable that the overall Pb isotope range, although more variable than that of the oceanic basalts with respect to *unradiogenic* $^{206}Pb/^{204}Pb$ and elevated Δ7/4, is otherwise generally associated with the field of the convecting mantle (Fig. 1).

Previously we have demonstrated that the Middle Atlas clinopyroxenes have strongly decoupled and unrealistic Δ7/4 and Δ8/4 systematics when modeled back in time (20–200 Myr). Fig. 8c–d illustrates the reverse experiment where samples Atl-3A, Atl-3K, Atl-3T Atl-3U are projected forward in time (200 Myr). Similar to the back-modeled evolution of these clinopyroxenes, Pb isotopes become rapidly decoupled from the associated NHRL (200 Myr). These compositions are very distinct from forward-projected "classic" HIMU-mantle. This poses interesting questions.

For example, why do a significant portion of SCLM minerals that have very high $^{232}Th/^{204}Pb$ and $^{238}U/^{204}Pb$ exhibit Pb isotopes akin to the convecting mantle? Moreover, why is there a general lack of very radiogenic, HIMU-like $^{206}Pb/^{204}Pb$ (>20.5) in the SCLM mineral record (Fig. 1). Given that some SCLM portions were stabilized in the Archean or Proterozoic, it should be expected that the evolution of Pb isotopes of these samples would result in distinctly more radiogenic Pb isotopes. Our measure of $^{206}Pb/^{204}Pb$ variability, the "$^{206}Pb/^{204}Pb$ indices" show that clinopyroxene suites

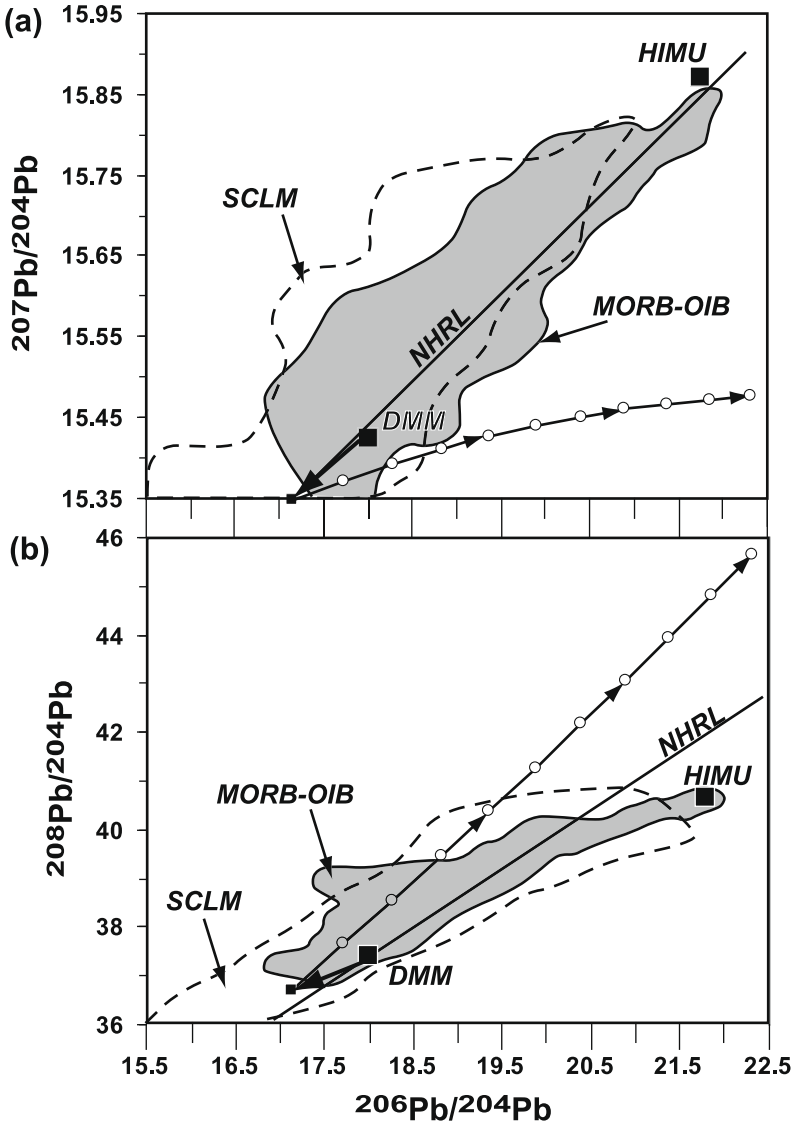

Fig. 9. Hypothetical evolution of DMM in $^{207}Pb/^{204}Pb$–$^{206}Pb/^{204}Pb$ (a) and $^{208}Pb/^{204}Pb$-$^{206}Pb/^{204}Pb$ (b) space. Present-day DMM is modeled 500 Myr back in time as indicated by the black arrow using μ and ω of 10 and 25 (small black square). This back-modeled DMM is then forward-projected with μ and ω of 75 and 375 for 500 Myr, respectively, in order to simulate the Pb isotope evolution if high-μ and high-ω clinopyroxenes, such as those from the Middle Atlas SCLM, were emplaced during metasomatism early in the Phanerozoic. The resulting Pb isotope compositions deviate substantially from the present-day NHRL, DMM, HIMU, the SCLM field and the MORB-OIB field. References for MORB-OIB (grey area) and SCLM fields (dashed outline) as well as the mantle endmembers are detailed in Fig. 1.

recovered from cratonic xenoliths (Cohen et al., 1984; Walker et al., 1989; Kramers et al., 1993; Carlson and Irving, 1994; Carlson et al., 2004) vary only between 0.4 and 4.9. Post-Archean SCLM hosts clinopyroxenes that result in "$^{206}Pb/^{204}Pb$ indices" between 0.3 and 3. It is evident that potentially ancient SCLM has only moderately more diverse Pb isotopes relative to much younger SCLM and both groups have Pb isotopes generally akin to the convecting mantle. Fig. 9 shows the Pb isotope evolution of hypothetical SCLM mantle akin to present-day DMM. This SCLM is age-corrected for 500 and 2800 Myr (not shown), and then forward-projected with high $^{232}Th/^{204}Pb$ and $^{238}U/^{204}Pb$ Pb (375 and 75, respectively) to the present-day, in order to simulate the effect of metasomatism, such as that experienced by the Middle Atlas peridotites, early in Earth's history. The resulting Pb isotope composition of the "Phanerozoic" model ($^{208}Pb/^{204}Pb$ ~45.7, $^{207}Pb/^{204}Pb$ ~15.48 and $^{206}Pb/^{204}Pb$ ~22.3, Fig. 9) is very different to the present-day range of MORB and OIB as well as SCLM. The "Archean" model produces even more extreme $^{206}Pb/^{204}Pb$ and $^{208}Pb/^{204}Pb$ of ~26.7 and 78.0 (not shown), respectively, that have never been observed in the convecting mantle.

There appears to be no evidence for different metasomatic mechanisms in Archean/Proterozoic SCLM compared with the Phanerozoic. In fact, the Sr–Nd–Hf isotope record of minerals from Archean SCLM principally require "normal" silicate-, hydrous, and/or carbonatitic metasomatism (e.g., Carlson and Irving, 1994; Simon et al., 2007) as proposed for the younger portions of continental and oceanic lithosphere (e.g., Lee et al., 1996; Downes, 2001; Ionov

et al., 2002; Bizimis et al., 2003, 2007; Pearson et al. 2003). However, we emphasize that two distinct selection processes might mask, or prevent, the observation of greater Pb isotope variation in SCLM.

Firstly, precursor liquids of the intra-plate volcanism might frequently "fertilize" the continental mantle roots imposing enrichment along a network of veins that later may be reactivated as pathways for asthenospheric melts on their way to the surface (e.g., Pilet et al., 2002, 2004; Jung et al., 2005). These passing melts could preferentially sample the metasomatised peridotitic vein-wall rocks in the form of xenoliths. Given that U, Th and Pb are among the least robust elements to the effects of metasomatism, the elemental and isotopic composition of the wall rocks would be efficiently modified. For example, we can assume the succession of metasomatic events in the Middle Atlas would have been reversed. Extreme carbonatitic fluids percolated the SCLM first and imparted the high $^{232}Th/^{238}U$, $^{232}Th/^{204}Pb$ and $^{238}U/^{204}Pb$ onto the clinopyroxenes. Then a later, subsequent passing of asthenospheric mafic silicate melts (or carbonatites with conventional μ, ω and κ) would have reset the elevated carbonatitic μ, ω and κ in this SCLM portion to the approximate values anticipated from the convecting mantle. These areas of the SCLM would than evolve parallel to the convecting mantle and never exhibit the extreme Pb isotope compositions modeled in Fig. 9. Considering that SCLM xenoliths are typically sampled by mafic silicate melts, that may metasomatise the SCLM during their ascent, the likelihood of sampling xenoliths with "asthenospheric" Pb isotopes and $^{232}Th/^{238}U$, $^{232}Th/^{204}Pb$ and $^{238}U/^{204}Pb$ systematics is very high. Importantly, it is difficult to anticipate the composition of SCLM distal from the volcanic centres, which escape metasomatism and sampling.

Secondly, further potential bias occurs when samples are chosen for isotopic analysis. Here, samples with high abundances of clinopyroxene are often preferred over more depleted, harzburgitic samples (i.e. less affected by metasomatism). This may enhance the sampling of variably metasomatised, but in terms of Pb isotopes "normal" SCLM clinopyroxenes. Therefore, Pb isotopes and systematics of SCLM clinopyroxenes might be considered as frequently reset, possibly during every tectonic/metasomatic event that allows silicate melts to percolate the SCLM, otherwise the asthenospheric Pb isotope record of the global SCLM data is difficult to envision and more extreme Pb isotope ratios as proposed in Fig. 9 should be more prevalent. However, apart from the "asthenospheric" Pb isotope record in SCLM minerals, the corresponding μ, ω and κ systematics are often distinct from the global record (Fig. 1). In the following section, we present a simple numerical model to show the range of μ and ω of basaltic melts that may be generated from fertile SCLM such as the Middle Atlas continental mantle root.

4.4. Putative basaltic melts generated from high μ–high ω SCLM clinopyroxenes

The Middle Atlas SCLM has a relatively fertile composition with high modal abundance of clinopyroxene (up to 23%, Wittig et al., in press). It could therefore act as a potential magma source as evidenced by the melt pockets found in some of these xenoliths. It is interesting to contemplate the μ and ω composition of these SCLM melts given the very high nature of these elemental ratios in the source clinopyroxenes. We present a melting model that is based on the non-modal fractional partial melting equations of Shaw (1970). Starting modal composition and melting proportions were taken from Wittig et al. (2006) and are given in Table 4. The partition coefficients for constituent minerals in spinel-facies peridotites were taken from Landwehr et al. (2001), Witt-Eickschen and O'Neill (2005), Hart and Gaetani (2006) and Wood et al. (1999) and are given in Table 5. For each of our Middle peridotites we show the μ and ω anticipated from pure basaltic melts generated after melting commenced to 0.5% and 1%, continuing thereafter in 1% increments to 10% (Fig. 10).

A first order observation from our model calculations is that due to the melting behavior of mantle pyroxenes and the very low pyroxene/silicate melt partition coefficients of U, Th and Pb (Wood et al., 1999; Landwehr et al., 2001), 99% of all U and Th is removed from the residual SCLM after only 2% melt extraction. With these parameters, U and Th fractionate from Pb during melting; resulting in elevated μ and ω relative to the original clinopyroxenes. Furthermore, is becomes clear that the melts generated at each melt increment have highly variable μ and ω (Fig. 10, Table A1). For example, after 0.5% melting of the Middle Atlas SCLM, melts are modeled with μ ranging from 216 to 691, while ω is more variable and ranges from 774 to 2267 (Fig. 10). After 10% depletion of the Middle Atlas SCLM, the corresponding magmas have μ ranging from 19 to 46, which is akin to the range observed from the convecting mantle and the host volcanic rocks. However, the Middle Atlas clinopyroxenes have high Th abundances and high ω and this combination yields modeled melts that are clearly off-set from the reference volcanic rocks (Fig. 10).

Table 4
Initial modal composition and melting proportions of primitive mantle used for melting calculations.

	Starting modal proportions			
	$X_{olivine}$	$X_{orthopyroxene}$	$X_{clinopyroxene}$	X_{spinel}
2 GPa	0.534	0.255	0.183	0.028
	Melting proportions			
	$P_{olivine}$	$P_{orthopyroxene}$	$P_{clinopyroxene}$	P_{spinel}
2 GPa	0.02	0.32	0.64	0.02

Table 5
Mineral/silicate melt partition coefficients used for melting calculations.

	U	Th	Pb
Mineral/basaltic melt partition coefficients			
Olivine	0.000018	0.000012	0
Orthopyroxene	0.0057	0.0022	0.2
Clinopyroxene	0.0170	0.022	0.2
Spinel	0	0	0

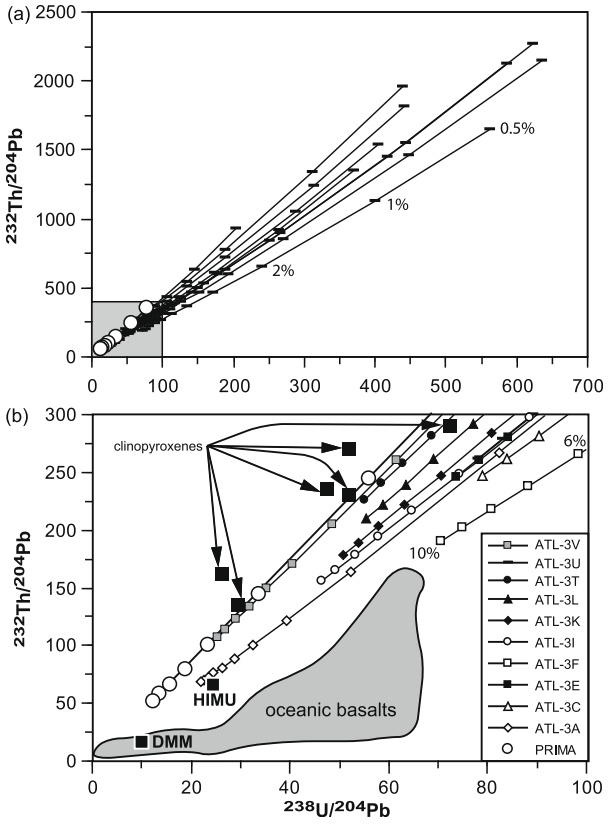

Fig. 10. $^{232}Th/^{204}Pb$ and $^{238}U/^{204}Pb$ composition of melt fractions (0.5–10%) modeled from the Middle Atlas clinopyroxenes using fractional melting equations after Shaw (1970), U, Th and Pb partition coefficients for clinopyroxene/melt from Landwehr et al. (2001) and clinopyroxene/orthopyroxene distribution after Witt-Eickschen and O'Neill (2005). Inset in (a) is shown in greater detail in (b). Typical compositions for DMM- and HIMU-mantle, the MORB-OIB array as well as the original clinopyroxenes from the Middle Atlas xenoliths are shown for comparison in (b). None of the Atlas xenoliths yield melts with suitably low $^{232}Th/^{204}Pb$ and $^{238}U/^{204}Pb$ to explain the composition of oceanic basalts and the intra-plate volcanic rocks.

The current melting model does not account for amphibole participation in the partial melting process. If amphibole is present during spinel-facies melting it is consumed almost instantaneously (LaTourette et al., 1995). In the Middle Atlas xenoliths amphibole is an accessory phase and therefore the calculated pure SCLM melts, particularly those of <2% melting, yield absolute minimum U, Th and Pb abundances and μ, ω and κ. For example, small-degree melting of Atl-3B and the presence of amphibole (0.8% modal abundance) would increase the μ and ω in a 0.5% melt from 691 and 2150 (clinopyroxene only) to 1050 and 2950, respectively.

These modeled μ and ω ratios of pure SCLM melts do show the potential for generating extreme μ and ω in melts and may present a finely tuned tool for tracing melts contributions from metasomatised SCLM to intra-plate volcanism that exceed the sensitivity of Sr, Nd and Hf isotopes. However, several mechanisms such as mixing "normal" asthenosphere magma or crustal components with high-μ and high-ω lithospheric melts as well as elemental fractionation during magma ascent might lower the originally elevated μ and ω ratios of pure SCLM melts; rendering the detection of SCLM contributions to terrestrial volcanism extremely difficult. Given the unremarkable nature of Sr, Nd and, in most cases, Hf isotopes in SCLM and the possible difficulties in preserving the elevated μ and ω found in some SCLM minerals, caution is warranted when SCLM is nominated as a discernible mantle component.

5. CONCLUSIONS

U, Th and Pb concentrations and ratios in combination with Pb isotope of mantle clinopyroxenes from the Middle Atlas SCLM provide insights into the timing of metasomatism, the prevalence and persistence of μ, ω and κ in the SCLM and the potential of detecting continental mantle root contributions to the isotopic diversity of volcanic rocks:

(1) Sr, Nd, Hf, Pb isotopes of our Middle Atlas clinopyroxenes are relatively homogeneous and show an affinity to HIMU. $^{232}Th/^{204}Pb$ and $^{238}U/^{204}Pb$ are extremely high and distinct from estimated values of oceanic basalt source mantle and those of the host intra-plate volcanic rocks. $^{87}Rb/^{86}Sr$, $^{147}Sm/^{143}Nd$ and $^{176}Lu/^{177}Hf$ are within the range of the convecting mantle.

(2) Elevated trace element abundances record metasomatic enrichment due to the percolation of carbonatitic fluids. Based on the μ, ω and κ and Pb isotopes, this metasomatism appears to be a very young, Cenozoic feature associated with, but clearly distinct from, the Quaternary intra-plate volcanism in the Middle Atlas.

(3) Globally, μ, ω and κ in SCLM appear to suggest that the restricted range of Pb isotopes generally does not originate from intrinsic time-integrated in-growth from their high $^{232}Th/^{204}Pb$ and $^{238}U/^{204}Pb$ over billions of years. Instead, the Pb isotopes of SCLM minerals tend to record very recent metasomatic events.

(4) Numerical modeling shows that putative basaltic melts generated from Middle Atlas SCLM may have extremely high μ and ω. These calculated values exceed those currently seen from oceanic basalts, although trace element fractionation during magma ascent and magma mixing may reconcile this discrepancy.

ACKNOWLEDGMENTS

This study was initially funded by a Danish National Research Foundation Grant to the Danish Lithosphere Centre (DK) and later benefited from NERC Grant NE/C5/9054/1 to D.G. Pearson (UK). N.W. is grateful for the hospitality and support provided by staff and students of the School of Geography, Environment and Earth Sciences, Victoria University of Wellington (NZ) in 2005. Martin Bizzarro and Toby Leeper are thanked for help with Pb and Sr isotope measurements in Copenhagen. Geoff Nowell and Chris Ottley helped with Hf and Nd isotope and trace element measurements in Durham. Jon Davidson, Christoph Beier and Karsten Haase are thanked for comments on an earlier version of this

paper. S.D. and K.H. were supported by the Deutsche Forschungsgesellschaft (DFG Grants DU426/1, DU426/3, HO1833/5, HO1833/6, HO 1833/18). The comments of two anonymous reviewers are appreciated and particularly the associated editor Mark Rehkämper helped to streamline the ideas presented in this contribution and to create a more palatable paper.

APPENDIX A

Table A1
U, Th and Pb concentrations (ppm) and $^{238}U/^{204}Pb$; $^{232}Th/^{238}U$; and $^{232}Th/^{204}Pb$ systematics of calculated melts produced from putative melting of Middle Atlas continental mantle.

	$^{238}U/^{204}Pb$	$^{232}Th/^{238}U$	$^{232}Th/^{204}Pb$	U	Th	Pb
	μ	κ	ω	ppm	ppm	ppm
Calculated 0.5% melt						
Atl-3A	216	3.6	774	2.327	8.061	0.713
Atl-3B	691	3.1	2150	13.187	39.695	1.268
Atl-3C	616	2.7	1661	9.499	24.786	1.025
Atl-3E	638	3.3	2122	10.259	33.007	1.066
Atl-3F	612	2.7	1651	9.499	24.786	1.025
Atl-3I	403	3.3	1347	2.179	7.048	0.356
Atl-3K	439	3.5	1538	5.769	19.552	0.875
Atl-3L	481	3.8	1813	9.384	34.253	1.298
Atl-3T	478	4.1	1953	15.581	61.608	2.173
Atl-3U	677	3.3	2267	10.312	33.428	1.014
Atl-3V	221	4.2	927	1.240	5.041	0.372
Average	497	3.4	1655	8.112	26.479	1.017
Calculated 2% melt						
Atl-3A	86	3.6	308	0.861	2.991	0.666
Atl-3B	272	3.1	848	4.880	14.729	1.183
Atl-3C	243	2.7	657	3.516	9.197	0.956
Atl-3E	253	3.3	844	3.797	12.248	0.995
Atl-3F	243	2.7	657	3.516	9.197	0.956
Atl-3I	160	3.4	536	0.806	2.615	0.333
Atl-3K	174	3.5	612	2.135	7.255	0.816
Atl-3L	191	3.8	721	3.473	12.710	1.211
Atl-3T	190	4.1	776	5.766	22.860	2.028
Atl-3U	268	3.4	901	3.816	12.404	0.946
Atl-3V	88	4.2	369	0.459	1.870	0.347
Average	197	3.4	657	3.002	9.825	0.949
Calculated 5% melt						
Atl-3A	40	3.6	143	0.348	1.210	0.580
Atl-3B	126	3.1	394	1.974	5.958	1.031
Atl-3C	113	2.7	305	1.422	3.720	0.833
Atl-3E	117	3.3	392	1.536	4.954	0.867
Atl-3F	113	2.7	305	1.422	3.720	0.833
Atl-3I	74	3.4	249	0.326	1.058	0.290
Atl-3K	81	3.5	284	0.864	2.935	0.712
Atl-3L	88	3.8	334	1.405	5.141	1.056
Atl-3T	88	4.1	360	2.332	9.247	1.767
Atl-3U	125	3.4	418	1.544	5.017	0.825
Atl-3V	41	4.2	171	0.186	0.757	0.303
Average	91	3.4	305	1.214	3.974	0.827
Calculated 10% melt						
Atl-3A	19	3.4	64	0.106	0.345	0.371
Atl-3B	66	3.0	197	0.683	1.986	0.688
Atl-3C	56	2.4	133	0.469	1.079	0.556
Atl-3E	74	3.3	245	0.768	2.477	0.692
Atl-3F	71	2.7	191	0.711	1.860	0.665
Atl-3I	46	3.4	156	0.163	0.529	0.231
Atl-3K	51	3.5	178	0.432	1.467	0.568
Atl-3L	55	3.8	210	0.702	2.571	0.843
Atl-3T	55	4.1	226	1.166	4.623	1.411
Atl-3U	78	3.4	262	0.772	2.509	0.658
Atl-3V	25	4.2	107	0.093	0.378	0.242
Average	54	3.4	179	0.551	1.802	0.630

REFERENCES

Abouchami W., Galer S. J. G. and Hofmann A. W. (2000) High precision lead isotope systematics of lavas from the Hawaiian Scientific Drilling Project. *Chem. Geol.* **169**, 187–209.

Ayarza P., Alvarez-Lobato F., Teixell A., Arboleya M. L., Tesón E., Julivert M. and Charroud M. (2005) Crustal structure under the High Atlas Mountains (Morocco) from geological and gravity data. *Tectonophysics* **400**, 67–84.

Bailey J. A. and Ragnarsdottir V. (1994) Uranium thorium solubilities in subduction zone fluids. *Earth Planet. Sci. Lett.* **124**, 1190129.

Baker J. A., Chazot G., Menzies M. A. and Thirlwall M. F. (1998) Metasomatism of the shallow mantle beneath Yemen by the Afar plume – implications for mantle plumes, flood volcanism, and intraplate volcanism. *Geology* **26**, 431–434.

Baker J. A., Peate D. W., Waight T. and Meyzen C. M. (2004) Pb isotopic analysis of standards and samples using a ^{207}Pb–^{204}Pb double spike and thallium to correct for mass bias with a double focusing MC-ICP-MS. *Chem. Geol.* **211**, 275–303.

Bedini R. M. and Bodinier J.-L. (1999) Distribution of incompatible trace elements between the constituents of spinel peridotite xenoliths: ICP-MS data from the East African Rift. *Geochim. Cosmochim. Acta* **63**, 3883–3900.

Becculuva L., Azzouni-Sekkal A., Benhallou A., Bianchini G., Ellam R. M., Marzola M., Siena F. and Stuart F. M. (2007) Intracratonic asthenosphere upwelling and lithosphere rejuvenation beneath the Hoggar swell (Algeria): evidence from HIMU metasomatised lherzolite mantle xenoliths. *Earth Planet. Sci. Lett.* **260**, 482–494.

Bell K. and Tilton G. R. (2001) Nd, Pb and Sr isotopic composition of East African carbonatites: evidence for mantle mixing and plume inhomogeneity. *J. Petrol.* **42**, 1927–1945.

Ben Othman D., Tilton G. R. and Menzies M. A. (1990) Pb, Nd, and Sr isotopic investigations of kaersutite and clinopyroxene from ultramafic nodules and their host basalts: the nature of subcontinental mantle. *Geochim. Cosmochim. Acta* **54**, 3449–3460.

Bizimis M., Griselin M., Lassiter J. C., Salters V. J. M. and Sen G. (2007) Ancient recycled mantle lithosphere in the Hawaiian plume: osmium–hafnium isotopic evidence from peridotite mantle xenoliths. *Earth Planet. Sci. Lett.* **257**, 259–273.

Bizimis M., Sen G. and Salters V. J. M. (2003) Hf–Nd isotope decoupling in the oceanic lithosphere: constraints from spinel peridotites from Oahu, Hawaii. *Earth Planet. Sci. Lett.* **217**, 43–58.

Bizzarro M., Baker J. A. and Ulfbeck D. (2003) A new digestion and chemical separation technique for rapid and highly reproducible determination of Lu/Hf and Hf isotope ratios in geological materials by MC-ICP-MS. *Geostand. Newslett.* **27**, 131–143.

Blichert-Toft J. and Albarede F. (1997) The Lu–Hf isotope geochemistry of chondrites and the evolution of the mantle–crust system. *Earth Planet. Sci. Lett.* **148**, 243–258.

Brandon A. D., Becker H., Carlson R. W. and Shirey S. B. (1999) Isotopic constraints on time scales and mechanisms of slab material transport in the mantle wedge: evidence from the Simcoe mantle xenoliths, Washington, USA. *Chem. Geol.* **160**, 387–407.

Carignan J., Ludden J. N. and Francis D. (1996) On recent enrichment of subcontinental lithosphere: a detailed U–Pb study of spinel lherzolite xenoliths, Yukon, Canada. *Geochim. Cosmochim. Acta* **60**, 4241–4252.

Carlson R. W. and Irving A. J. (1994) Depletion and enrichment history of subcontinental lithospheric mantle: an Os, Sr, Nd and Pb isotopic study of ultramafic xenoliths from the northwestern Wyoming Craton. *Earth Planet. Sci. Lett.* **126**, 457–472.

Carlson R. W., Irving A. J., Schulze D. J. and Hearn J. B. C. (2004) Timing of Precambrian melt depletion and Phanerozoic refertilization events in the lithospheric mantle of the Wyoming Craton and adjacent Central Plains Orogen. *Lithos* **77**, 453–472.

Charlier B. L. A., Ginibre C., Morgan D., Nowell G. M., Pearson D. G., Davidson J. and Ottley C. J. (2006) Methods for the microsampling and high-precision analysis of strontium and rubidium isotopes at single crystal scale for petrological and geochronological applications. *Chem. Geol.* **232**, 114–133.

Chauvel C. and Jahn B. M. (1984) Nd–Sr isotope and REE geochemistry of alkali basalts from the Massif Central, France. *Geochim. Cosmochim. Acta* **48**, 93–110.

Choi S. H., Kwon S.-T., Mukasa S. B. and Sagong H. (2005) Sr–Nd–Pb isotope and trace element systematics of mantle xenoliths from late Cenozoic alkaline lavas, South Korea. *Chem. Geol.* **221**, 40–61.

Cohen R. S., O'Nions R. K. and Dawson J. B. (1984) Isotope geochemistry of xenoliths from East Africa: implications for development of mantle reservoirs and their interaction. *Earth Planet. Sci. Lett.* **68**, 209–220.

Davidson J. P., Charlier B., Hora J. M. and Perlroth R. (2005) Mineral isochrons and isotopic fingerprinting: pitfalls and promises. *Geology* **33**, 29–32.

Downes H. (2001) Formation and modification of the shallow subcontinental lithospheric mantle: a review of geochemical evidence from ultramafic xenolith suites and tectonically emplaced ultramafic massifs of the Western and Central Europe. *J. Petrol.* **42**, 233–250.

Duggen S., Hoernle K., van den Bogaard P., Ruepke L. and Morgan J. P. (2003) Deep roots of the Messinian salinity crisis. *Nature* **422**, 602–604.

Duggen S., Hoernle K., Hauff F., Kluegel A., Bouabdellah M. and Thirlwall M. F. (2009) Flow of Canary mantle plume mantle material through a sub-lithospheric corridor beneath Africa to the Mediterranean. *Geology* **37**, 283–286.

Duggen S., Hoernle K., Kluegel A., Geldmacher J., Thirlwall M., Hauff F., Lowry D. and Oates N. (2008) Geochemical zonation of the Miocene Alboran Basin volcanism (westernmost Mediterranean): geodynamic implications. *Contrib. Mineral. Petrol.* **156**, 577–593.

El Azzouzi M., Bernard-Griffiths J., Bellon H., Maury R., Piqué A., Fourcade S., Cotten J. and Hernandez J. (1999) Évolution des sources du volcanisme marocain au cours du Néogène. *C.R. Acad. Sci. IIA* **329**, 95–102.

Galer S. J. G. (1999) Optimal double and triple spiking for high precision lead isotopic measurements. *Chem. Geol.* **157**, 255–274.

Galer S. J. G. and O'Nions R. K. (1985) Residence time of thorium, uranium and lead in the mantle with implications for mantle convection. *Nature* **316**, 778–782.

Galer S. J. G. and O'Nions R. K. (1989) Chemical and isotopic studies of ultramafic inclusions from the San Carlos Volcanic Field, Arizona: a bearing on their petrogenesis. *J. Petrol.* **30**, 1033–1064.

Gomez F., Allemendiger R. B. M., Er-Raji A. and Dahmani M. (1998) Crustal shortening and vertical strain partitioning in the Middle Atlas Mountains of Morocco. *Tectonics* **17**, 520–533.

Hamelin B. and Allègre C. J. (1988) Lead isotope study of orogenic lherzolite massifs. *Earth Planet. Sci. Lett.* **91**, 117–131.

Hanan B. B., Blichert-Toft J., Kingsley R., Schilling J. G. (1999) Depleted Iceland mantle plume geochemical signature: artefact or multicomponent mixing. *Geochem. Geophys. Geosys.* **1**, GC000009.

Harlou R., Pearson D. G., Nowell G. M., Ottley C. J. and Davidson J. (2009) Combined Sr isotope and trace element

analysis of melt inclusions at sub-ng levels using micro-milling techniques. *Chem. Geol.* **260**, 254–268.

Hart S. R. (1984) A large-scale isotope anomaly in the southern hemisphere mantle. *Nature* **309**, 753–757.

Hart S. R. and Gaetani G. A. (2006) Mantle Pb paradoxes: the sulfide solution. *Contrib. Mineral. Petrol.* **152**, 295–308.

Hassler D. R. and Shimizu N. (1998) Osmium isotopic evidence for ancient subcontinental lithospheric mantle beneath the Kerguelen Islands, Southern Indian Ocean. *Science* **280**, 418–421.

Hauri E. H., Wagner T. P. and Grove T. L. (1994) Experimental and natural partitioning of Th, U, Pb and other trace elements between garnet, clinopyroxene and basaltic melts. *Chem. Geol.* **117**, 149–166.

Hawkesworth C. J., Erlank A. J., Marsh J. S., Menzies M. A. and van Calsteren P. W. C. (1983) Evolution of the continental lithosphere: evidence from volcanics and xenoliths from southern Africa. In *Continental Basalts and Mantle Xenoliths* (eds. C. J. Hawkesworth and M. J. Norry). Shiva.

Hofmann A. W. (1997) Mantle geochemistry: the message from oceanic volcanism. *Nature* **385**, 219–229.

Ionov D. A., Bodinier J.-L., Mukasa S. B. and Zanetti A. (2002) Mechanisms and sources of mantle metasomatism: major and trace element compositions of peridotite xenoliths from Spitsbergen in the context of numerical modelling. *J. Petrol.* **43**, 2219–2259.

Jacobsen S. B. and Wasserburg G. J. (1980) Sm-Nd isotopic evolution of chondrites. *Earth and Planetary Science Letters* **50**, 139–155.

Johnson C. M. and Beard B. L. (1993) Evidence from hafnium isotopes for ancient sub-oceanic mantle beneath the Rio Grande rift. *Nature* **362**, 441–444.

Jung S., Pfaender J. A., Bruegmann G. and Stracke A. (2005) Source of primitive alkaline volcanic rocks from the Central European Volcanic Province (Rhoen, Germany) inferred from Hf, Pb and Os isotopes. *Contrib. Mineral. Petrol.* **150**, 546–559.

Knight K. B., Nomade S., Renne P. R., Marzoli A., Bertrand H. and Youbi N. (2004) The Central Atlantic Magmatic Province at the Triassic–Jurassic boundary: Paleomagnetic and $^{40}Ar/^{39}Ar$ evidence from Morocco for brief, episodic volcanism. *Earth Planet. Sci. Lett.* **228**, 143–160.

Kramers J. D., Roddick J. C. M. and Dawson J. B. (1993) Trace element and isotope studies on veined, metasomatic and "MARID" xenoliths from Bulfontein, South Africa. *Earth Planet. Sci. Lett.* **65**, 90–106.

Landwehr D., Blundy J. D., Chamorro-Perez E. M., Hill E. and Wood B. J. (2001) U-series disequilibria generated by partial melting of spinel lherzolite. *Earth Planet. Sci. Lett.* **188**, 239–348.

LaTourette T., Hervig R. L. and Holloway J. R. (1995) Trace element partitioning between amphibole, phlogopite, and basanite melt. *Earth Planet. Sci. Lett.* **135**, 13–30.

Lee D.-C., Halliday A. N., Davies G. R., Essene E. J., Fitton J. G. and Temdjim R. (1996) Melt enrichment of shallow depleted mantle: a detailed petrological, trace element and isotopic study of mantle-derived xenoliths and megacrysts from the Cameroon Line. *J. Petrol.* **37**, 415–441.

Malarkey J., Pearson D. G., Davidson J., Wittig N. (2008) Origin of Cr-diopside in peridotite xenoliths: recent metasomatic addition revealed by a micro-sampling, trace element and Sr isotopic study of on-craton and off-craton peridotites. In *9th International Kimberlite Conference*. Extended Abstract No. 9IKC-A-00133.

McKenzie D. P. and O'Nions R. K. (1983) Mantle reservoirs and oceanic basalts. *Nature* **301**, 229–231.

McKenzie D. P. and O'Nions R. K. (1995) The source regions of ocean island basalts. *Journal of Petrology* **36**, 133–159.

Meijer A., Kwon T.-T. and Tilton G. R. (1990) U–Th–Pb partitioning behaviour during partial melting in the upper mantle: Implications for the origin of high-mu components and the "Pb paradox". *J. Geophys. Res.* **95**, 433–448.

Mukasa S. B. and Shervais J. W. (1999) Growth of subcontinental lithosphere: evidence from repeated dike injections in the Balmuccia lherzolite massif, Italian Alps. *Lithos* **48**, 287–316.

Mukasa S. B., Shervais J. W., Wilshire H. G. and Nielson J. E. (1991) Intrinsic Nd, Pb and Sr isotopic heterogeneities exhibited by the Lherz alpine peridotite massif, French Pyrenees. *J. Petrol.* **117**, 134.

Nowell G. M., Pearson D. G., Ottley C. J., Schwieters J. and Dowall D. P. (2003) Long-term performance characteristics of a plasma ionisation multi-collector mass spectrometer (PIMMS): the ThermoFinnigan Neptune. In *Plasma Source Mass Spectrometry, Applications and Emerging Technologies* (ed. J. G. H. S. D. Tanner). Royal Society of Chemistry, Cambridge.

O'Reilly S. Y., Zhang M., Griffin W. L., Begg G., Hronsky J. (2006) Ancient lithosphere domains in ocean basins are key geochemical "reservoirs". In *Goldschmidt Conference*. Elsevier, Melbourne.

O'Reilly S. Y., Griffin W. L., Zhang M., Begg G. (2008) Archean Lithospheric mantle: its formation, its composition and today's refertilized remains. In *9th International Kimberlite Conference*. Extended Abstract No. 9IKC-A-00033.

Ottley C. J., Pearson D. G. and Irvine G. J. (2003) A routine procedure for the analysis of REE and trace elements in geological samples by ICP-MS. In *Plasma Source Mass Spectrometry: Applications and Emerging Technologies* (eds. J. G. Holland and S. D. Tanner). Royal Society of Chemistry, Cambridge.

Pearson D. G., Davies G. R. and Nixon P. H. (1993) Geochemical constraints on the petrogenesis of diamond facies pyroxenites from the Beni Bousera Massif, North Morocco. *J. Petrol.* **34**, 125–172.

Pearson D. G. and Nowell G. M. (2002) The continental lithospheric mantle: characteristics and significance as a mantle reservoir. *Philos. Trans. Roy. Soc. Lond.* **360**, 2383–2410.

Pearson D. G., Canil D. and Shirey S. B. (2003) Mantle samples included in volcanic rocks: xenoliths and diamonds. In *Treatise on Geochemistry* (eds. H. D. Holland and K. K. Turekian). Elsevier, Amsterdam.

Pearson D. G. and Nowell G. M. (2004) Re–Os and Lu–Hf isotopes constraints on the origin and age of pyroxenites from the Beni Bousera peridotite massif: implications for mixed peridotite–pyroxenite mantle sources. *J. Petrol.* **45**, 439–455.

Pilet S., Hernandez J., Bussy F. and Sylvester P. J. (2004) Short-term metasomatic control of Nb/Th ratios in the mantle sources of intraplate basalts. *Geology* **32**, 113–116.

Pilet S., Hernandez J. and Villemant B. (2002) Evidence for high silicic melt circulation and metasomatism events in the mantle beneath alkaline provinces: the Na–Fe–augitic green-core pyroxenes in the tertiary alkali basalts of the Cantal massif (French Massif Central). *Mineral. Petrol.* **76**, 39–62.

Porcelli D. R., O'Nions R. K., Galer S. J. G., Cohen A. S. and Mattey D. P. (1992) Isotopic relationships of volatile and lithophile trace elements in continental ultramafic xenoliths. *Contrib. Mineral. Petrol.* **110**, 528–538.

Rosenbaum J. M., Wilson M. and Downes H. (1997) Multiple enrichment of the Carpathian–Pannonian mantle: Pb–Sr–Nd isotope and trace element constraints. *J. Geophys. Res.* **102**, 14947–14961.

Santos J. F., Schärer U., Ibarguchi J. I. G. and Girardeau J. (2002) Genesis of pyroxenite-rich peridotite at Cabo Ortegal (NW Spain): geochemical and Pb–Sr–Nd isotope data. *J. Petrol.* **43**, 17–43.

Shaw D. M. (1970) Trace element fractionation during anatexis. *Geochim. Cosmochim. Acta* **34**, 237–243.

Shaw J. E., Baker J. A., Kent A. J. R., Ibrahim K. M. and Menzies M. A. (2007) Chemical and isotopic character of Arabian lithospheric mantle—a source for intraplate volcanism? *J. Petrol.* **48**, 1495–1512.

Simon N., Carlson R. W., Pearson D. G. and Davies G. R. (2007) The origin and evolution of the Kaapvaal cratonic lithospheric mantle. *J. Petrol.* **48**, 589–625.

Steiger R. H. and Jager E. (1977) Submission on geochronology: convention of the use of decay constants in geo- and cosmochronology. *Earth Planet. Sci. Lett.* **36**, 359–362.

Stolz A. J. and Davies G. R. (1988) Chemical and isotopic evidence from spinel lherzolite xenoliths for episodic metasomatism of the upper mantle beneath Southeast Australia. *J. Petrol.* **Special Lherzolite issue**, 303–330.

Stracke A., Bizimis M. and Salters V. J. M. (2003) Recycling oceanic crust: quantitative constraints. *Geochem. Geophys. Geosyst.* **4**, 1–33.

Sun S.-s. and McDonough W. F. (1989) Chemical and isotopic systematics of oceanic basalts: implications for mantle composition and processes. In *Magmatism in the Ocean Basins* (eds. A. D. Saunders and M. J. Norry). Geological Society Special Publications, London.

Tatsumoto M., Basu A. R., Wankang H., Junwen W. and Guanghong X. (1992) Sr, Nd, Pb isotopes of ultramafic xenoliths in volcanic rocks of Eastern China: Enriched components EM I and EM II in subcontinental lithosphere. *Earth Planet. Sci. Lett.* **113**, 107–128.

Tatsumoto M., Knight R. J. and Allègre C. J. (1973) Time difference in the formation of meteorites as determined from the ratio of lead-207 to lead-206. *Science* **180**, 1279–1283.

Tera F. (2006) Lead isotope planetary profiling (LIPP): summation-depiction of Earth's many reservoirs. *Chem. Geol.* **233**, 1–45.

Thirlwall M. F. (1997) Pb isotopic and elemental evidence for OIB derivation from young HIMU mantle. *Chem. Geol.* **139**, 51–74.

Thirlwall M. F. (2000) Inter-laboratory and other errors in Pb isotope analyses investigated using a ^{207}Pb–^{204}Pb double spike. *Chem. Geol.* **163**, 299–322.

Thirlwall M. F. (2002) Multicollector ICP-MS analysis of Pb isotopes using a $^{207}Pb/^{204}Pb$ double spike demonstrates up to 400ppm/amu systematic errors in Tl-normalization. *Chem. Geol.* **184**, 255–279.

Turner S. and Hawkesworth C. J. (1995) The nature of the subcontinental mantle: constraints from the major-element composition of continental flood basalts. *Chem. Geol.* **120**, 295–314.

Ulfbeck D., Baker J. A., Waight T. and Krogstad E. (2003) Rapid sample digestion by fusion and chemical separation of Hf for isotopic analysis by MC-ICPMS. *Talanta* **59**, 365–373.

Verati C., Bertrand H. and Féraud G. (2005) The farthest record of the Central Atlantic Magmatic Province into West African Craton: precise $^{40}Ar/^{39}Ar$ dating and geochemistry of Taoudenni basin intrusives (Mali). *Earth Planet Sci. Lett.* **235**, 391–407.

Walker R. J., Carlson R. W., Shirey S. B. and Boyd F. R. (1989) Os, Sr, Nd, and Pb isotope systematics of southern African peridotite xenoliths: implications for the chemical evolution of subcontinental mantle. *Geochim. Cosmochim. Acta* **53**, 1583–1595.

Walter M. J. (2003) Melt extraction and compositional variability in mantle lithosphere. In *Treatise on Geochemistry* (eds. H. D. Holland and K. K. Turekian). Elsevier.

Witt-Eickschen G. and O'Neill S. C. (2005) The effect of temperature on the equilibrium distribution of trace elements between clinopyroxene, orthopyroxene, olivine and spinel in upper mantle peridotite. *Chem. Geol.* **221**, 65–101.

Witt-Eickschen G., Seck H. A., Mezger K., Eggins S. M. and Altherr R. (2003) Lithospheric mantle evolution beneath the Eifel (Germany): constraints from Sr–Nd–Pb isotopes and trace element abundances in spinel peridotite and pyroxenite xenoliths. *J. Petrol.* **44**, 1077–1095.

Wittig N. (2006) Application of novel U–Th–Pb and Lu–Hf isotopic techniques to tracing the melting and metasomatic history of mantle rocks. Ph.D. thesis, Danish Lithosphere Centre, Copenhagen University, pp. 1–351.

Wittig N., Baker J. A. and Downes H. (2006) Dating the mantle roots of young continental crust. *Geology* **34**, 237–240.

Wittig N., Baker J. A. and Downes H. (2007) U–Th–Pb and Lu–Hf isotopic constraints on the evolution of sub-continental lithospheric mantle, French Massif Central. *Geochim. Cosmochim. Acta* **71**, 1290–1311.

Wittig N., Pearson D. G., Baker J. A. and Downes H. (2009a) The U, Th and Pb elemental and isotopic compositions of mantle clinopyroxenes and their grain boundary contamination derived from leaching and digestion experiments. *Geochim. Cosmochim. Acta* **73**, 469–488.

Wittig N., Pearson D. G., Baker J. A., Duggen S., Hoernle K. (2008) Young continental mantle root beneath the Middle Atlas, Morocco: Evidence for carbonatite metasomatism. In *9th International Kimberlite Conference*. Extended Abstract No. 9IKC-A-00168.

Wittig N., Pearson D. G., Baker J. A., Duggen S., Hoernle K. (in press) A major element, PGE and Re-Os isotope study of Middle Atlas (Morocco) peridotite xenoliths: evidence for coupled introduction of metasomatic sulphides and clinopyroxene. *Lithos*. doi:10.1016/j.lithos.2009.11.003.

Wood B. J., Blundy J. D. and Robinson J. A. C. (1999) The role of clinopyroxene in generating U-series disequilibrium during mantle melting. *Geochim. Cosmochim. Acta* **63**, 1613–1620.

Woodhead J. D., Volker F. and McCulloch M. T. (1995) Routine lead isotope determinations using a lead-207–lead-204 double spike: a long-term assessment of analytical precision and accuracy. *Analyst* **120**, 35–39.

Associate editor: Mark Rehkamper